3 The Theory Behind the Conversion of Ocean Wave Energy: a Review

Gareth Thomas

Dept. of Applied Mathematics
University College Cork
Cork
Ireland

3.1 Introduction

The development of any new device is usually accompanied by extravagant claims that it has the potential to solve all of (or more modestly, a significant percentage of) the world's (or a nation's) energy problems. The inventor's strategy is usually to insist that the basic device is a magnificent absorber of energy, inexpensive to construct, resilient enough to survive the most violent storms and, if placed in rows or arrays around the coastline, the sum of the total output would provide the claimed power output. In the unlikely circumstance that all potential structural engineering problems have been solved, permissions granted and that grid connection really is a mere formality, then there are three simple modelling considerations that obstruct immediate success. These are in addition to host other practical obstacles that quickly arise.

The fundamental optimal performance of any device, based upon optimal performance criteria, usually counters any widely excessive claims being validated. Arrays of devices are subject to rather surprising constraints and will almost always not behave in the way they are intended to do. The third is concerned with wave climate and device design; site resource is an important consideration in device design and this is not rarely included in a preliminary implementation plan. All three are crucial aspects of device awareness and provide major pitfalls for newcomers to the field! In the present context, the question to be addressed is how these restrictions came to be known. An attempt is made within this review to provide an explanation as to these results were obtained, how they may be employed in a beneficial sense and the importance of designing a device to match the wave climate.

3.1.1 Historical and Parallel Perspectives

The pioneering work on the mathematical modelling of *Wave Energy Converters* (WECs) assumed that the waves were of small amplitude, relative to both the wavelength and the water depth, and of permanent regular form (the basic hypotheses of linear wave theory). These two assumptions permitted the extensive body of work that already existed in the fields of ship hydrodynamics and offshore structures, which are combined here under the umbrella heading of *Marine Hydrodynamics*, to be utilised immediately. Skilled practitioners became enthusiastic about the proposed technology and applied their expertise to wave energy utilisation, although the transfer of the existing theory to wave energy was itself a major task. This enabled important global results, such as the maximum power that a WEC could extract in one or more modes of motion, to be established at a very early stage. Such global modelling results have played an important part in assessing the behaviour and hydrodynamic viability of devices. In a similar manner, numerical methods developed in marine hydrodynamics have proved beneficial in wave energy applications.

The continuing importance of marine hydrodynamics to both commercial and military interests has ensured that as both theory and numerical modelling have developed, they have done so with obvious benefit to the wave energy community.

There is another aspect too. Marine hydrodynamics has progressed with both theory and experiment playing important roles. Substantial and comprehensive programmes have been implemented to develop experimental facilities with the intention of validating theoretical or numerical predictions. This has been to the obvious benefit of wave energy; it allows physical scale models to be built both with confidence and with an understanding of the strengths and limitations of the experimental testing programme.

If there has been a disadvantage associated with the maritime link, it is that the power take-off and associated technologies have not been developed at the same pace as the hydrodynamic modelling. Whilst this deficiency is now being addressed, there remains a slightly skewed approach with perhaps an over-emphasis upon the hydrodynamic input rather than the controlled output.

3.1.2 Scope of the Review

There are a surprisingly wide range of devices and it is not possible to consider each individually within a short review, nor is it possible or desirable to concentrate solely upon a single device or a family of devices. A good summary of device operation and status is given by Brooke (2003) and much more detailed information can be obtained from the accompanying chapters of this volume. The intent is to focus upon generic modelling from a hydrodynamic perspective with the aim of presenting the conversion process in as uniform a manner as possible over all families of devices. Applications will be given wherever possible but the focus is upon the broad concepts of operation and design.

A detailed knowledge of wave mechanics or hydrodynamics is not assumed but some knowledge of oscillating mechanical systems is considered desirable. The approach adopted is to provide a general background to the subject initially and then progress to the application of modelling wave energy devices. One of the principal needs of the newcomer is to acquire a working knowledge of the requisite maritime and hydrodynamic disciplines and this is addressed by identifying the appropriate textbooks in the distinct specialities. The fundamental modelling strategies and results are referenced to the key papers in the discipline and the few existing review articles are referenced whenever possible.

In terms of structure, a broad description of the terminology and concepts is given first and followed by a description of the resource to enable the conversion challenge and environment to be identified. A restriction to floating devices is then enforced, enabling the broad concepts of hydrodynamic modelling, optimal power absorption, control and design to be described for generic categories of devices. The review is completed by a final section on the modelling of the *Oscillating Water Column* (OWC) device, given separately to indicate its historical dominance presently in application and instalment but also in recognition of its distinctive modelling requirements. Analogies in approaches and results between the various sections are drawn whenever possible.

One limiting restriction is imposed throughout and this concerns permissible power take-off systems: only those devices that operate by utilising the oscillatory nature of resource directly are considered. The principle class of devices excluded is comprised of those devices, floating or fixed, that employ an overtopping principle and collecting chamber. Such a restriction is reasonable when an emphasis is placed upon time-dependent wave fields and motions.

3.2 Terminology and Concepts

3.2.1 Conversion Terminology

The standard terminology illustrates the strengths and weaknesses of WEC modelling. Many of the original concepts and terminology introduced in the 1970s remain in common use and this itself a tribute to the very high quality of the early work although others indicate perhaps a common lack of understanding at that time.

For an isolated body in three dimensions, the fundamental quantity employed to evaluate device performance is the *Capture Width*. At a given frequency this is defined to be the ratio of the total mean power absorbed by the body to the mean power per unit crest wave width of the incident wave train, where *mean* refers to the average value per wave period for regular waves or per energy period for irregular waves. Some early papers employ the descriptor *Absorption Length* or *Absorption Width* in place of capture width. Capture width has the dimension of

length and sometimes the non-dimensional measure denoting the ratio of the capture width to the width of the device is a useful quantity to assess device performance. There is no standard term to indicate this quantity and *Non-dimensional Capture Width*, *Relative Capture Width* and *Non-dimensional Absorption Length* have all been used.

The two-dimensional historical analogue of capture width is *Efficiency* and this has played an important role in laboratory comparisons of theory and experiment in narrow wave tanks. Additionally, it is usually easier to develop two-dimensional numerical models rather than three-dimensional ones and this has also played a role in the adopting the given notation. It may seem that efficiency and relative capture width are similar non-dimensional measures but this is not the case. Efficiency is the ratio of output power to input power for a two-dimensional system, with a unit width of the device able to extract power from only a unit width of the incident wavefront; thus it has a maximum value of unity, more often quoted as a maximum percentage value of 100 %. The relative capture width may possess a value of greater than one, as three-dimensional effects permit the device to absorb power from the total wavefront incident upon the device and not restricted to a wavefront possessing just the same width as the device. Both capture width and efficiency were originally derived for regular waves and have been extended readily to irregular waves.

Within the broader remit of wave energy extraction, the definition of capture width remains unambiguous but this is not true for efficiency. It is possible to provide a number of definitions of efficiency, based upon the consideration of various measures of the total system or particular subsystems. To avoid confusion, the traditional use of efficiency from a hydrodynamic perspective will be labelled the *Hydrodynamic Efficiency* and is the quantity considered in this review. This permits the single word *Efficiency* to follow the more general definition of the ratio of power output to power absorbed, related to the practical implementation and no longer restricted to two dimensions.

The *Maximum Capture Width* of a device of specified geometry, at a given frequency, is obtained by optimising the capture width with respect to the parameters of the power take-off mechanism. This corresponds to the mean absorbed power taking its maximum value and this will generally be strongly frequency dependent. In linear theory the power take-off mechanisms are often modelled by black-box models in which the system is represented by an applied linear damping term.

If a device is tuned to operate optimally at a specified frequency, then this will determine the power take-off parameters and the *Bandwidth* curve is found by plotting the capture width against frequency for the fixed power take-off parameters. This will coincide with the maximum capture width at the tuning frequency but not generally at other frequencies, when the values on the bandwidth curve will usually be below the maximum capture width. The character of the bandwidth curve is an important indicator of the device performance: a broad bandwidth suggests that the device will work well over a wide range of conditions, whereas a narrow bandwidth suggests that its performance capabilities will be good close to the tuning frequency but poor elsewhere.

3.2.2 Classification of Devices

Early work was targeted primarily at floating devices and typically classified a given device as being a *Point Absorber*, a *Terminator* or an *Attenuator* and the descriptors are still used to a certain extent. They are intended to describe the principle of operation and provide information on the geometry of the device and are shown schematically in Fig. 3.1. *Point Absorbers* are devices, usually axisymmetric about a vertical axis, which are small in the sense that the horizontal physical dimensions of the device are small relative to the wavelength of the incident waves. The concept of such a device is very appealing from a modelling viewpoint because the scattered wave field can be neglected and forces on the body are only due to the incident waves. Point absorbers are capable of absorbing the energy from a wavefront many times the key horizontal dimension of the absorber and so possess a large potential capture width. The theory predicts that such a performance can only be achieved if the device undergoes oscillations whose magnitude may be many times that of the incident wave amplitude. This behaviour is not permissible in practice and has led to the development of theories, not solely restricted to point absorbers, to predict the maximum capture width when the amplitude of the device oscillation is constrained in magnitude but permitted to maintain the frequency of oscillation.

Attenuators and *Terminators* are WECs which have finite dimensions relative to the incident wave field and moreover have one dominant horizontal dimension. A simple way to envisage the concept in plan is to consider a rectangle or ellipse that has a much greater length than breadth. *Attenuators* are aligned with the incident wave direction with their beam much smaller than their length and *Terminators* are positioned with the dominant direction perpendicular to the incident waves, with beam much greater than length. It is usual for attenuators to be compliant or articulated structures and often the initial design concept was that the waves would attenuate along the device as power was extracted; this concept is generally incorrect and the motion of the attenuator may be almost symmetric about the mid-point of the device, so that the fore and aft portions of the device work equally hard. Terminators can be rigid or compliant. There is little hydrody-

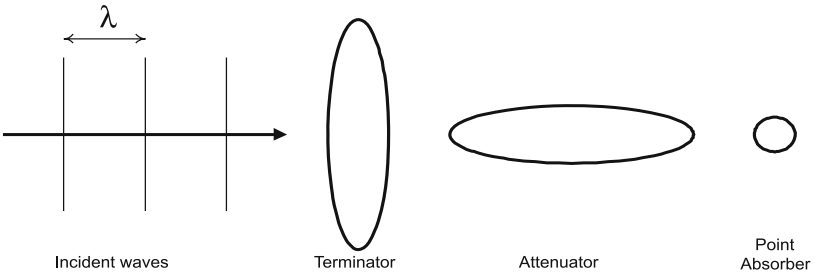

Fig. 3.1. Schematic showing scale and orientation of a *Terminator*, *Attenuator* and *Point Absorber*

namic difference in the behaviour of a compliant terminator and attenuator; it is essentially that the incident wave directions differ by a right angle. This illustrates an important point: the mode of operation is linked closely to the incident wave field and this will vary. Without controlling mechanisms, an elongated device could be forced to act as an attenuator or a terminator at the same site and different sea states. The alignment process is linked to the mooring configuration and this identifies one of the key requirements of the moorings for a WEC. It may not be sufficient for the mooring(s) to ensure that a device is maintained at a selected site, the mooring may also be required to ensure device alignment as well. In this context, it is salient to make that observation that an elongated device in attenuator mode will usually experience considerably lower mooring forces than the same device on terminator mode.

3.2.3 Alternative Device Classification

The classification system above is targeted at floating devices but this is not sufficient if all device categories are to be encompassed. For example, the first successful OWCs were introduced by Masuda, as described by Brooke (2003), and these are genuine residents of the point absorber family. More recent OWCs have been shore-mounted; any shore-mounted device can be described as a terminator but there are obvious differences between devices onshore and offshore. Thus although the usual method of classifying wave energy devices is based upon the mode of operation primarily, it is often informative to add one or more qualifiers to describe the device, its proposed method of working and intended site. Thus, for example, the descriptor *Oscillating Water Column* (OWC) describes how the device operates but does not provide information concerning the location where the device would best be employed. This shortcoming can be remedied by the inclusion of an additional qualifier, such as *Onshore*, *Nearshore* or *Offshore,* to specify the location.

For the present purpose it is expedient to use a slightly different classification system to the physically precise one outlined previously; the new system was developed in the EU-funded OWEC-1 project and reported by Randløv (1996). This classification is based upon the present status of a device, the development timescale and economic investment cost; the mode of operation is not used as a defining quantity. If these new considerations are utilised, then any device can be classified as being a *First Generation System*, a *Second Generation System* or a *Third Generation System*. The three categories are not mutually exclusive and share common features; this difficulty is acknowledged but further details will not be discussed.

Onshore or nearshore OWC devices are considered to be *First Generation Systems* and such devices are installed presently or under development in the UK, Portugal, India and Japan. The dominance of OWCs partly reflects an ability to build such devices with conventional technology and power take-off equipment, although this remark is tempered by the fact that considerable development work has been required in both technology and power take-off. In some sense, OWCs

are the most difficult to model of the three categories, as confirmed in Section 3.7, and considerable modelling effort is still required.

Second Generation Systems, represented by float pumps, are designed to operate at a wide variety of offshore and nearshore sites where high levels of energy are available. Installation is usually considered possible in water depths of between thirty and a hundred meters. Float pumps may be slack-moored or tight-moored but all possess a favourable ratio between absorbed energy and volume. They clearly do not represent, nor are intended to represent, all future categories of offshore devices, but these devices are relatively small both in physical size and power output; as such they are ideal for a relatively short and inexpensive development period. These devices belong to the point absorber category as the horizontal physical dimensions of the device are much smaller than the wavelength of the waves from which the device is designed to extract energy. It is worth noting that it is not always possible to make an additional classification based upon power take-off characteristics. Innovative hydraulic machines promise power take-off systems with a means of energy storage and increased power output by control of device motion for some devices, whereas others are essentially offshore floating OWCs with a pneumatic power take-off mechanism.

The defining property of *Third Generation Systems* is that they are large-scale offshore devices, both in terms of physical size and power output. Such advanced systems could well be seen as the final stage of device development following the successful implementation of float pump systems. It is important to recognise that a large power output is attainable potentially from either a single device of large physical dimensions or a large array of devices, which individually are of much smaller size. Large single devices correspond to the terminators and attenuators of the device classification standard adopted in Section 3.2.2 and an array of smaller float-type devices requires the array theories described in Section 3.4.

Any proposed classification system cannot be entirely satisfactory and the task is riddled with difficulties. The Pelamis device described in Chapter 7 can be considered as an attenuator with regard to the initial classification system and as a third generation device in the context of the alternative classification. Thus both first and third generation devices have been installed and deployed successfully but no second generation device has yet been awarded similar status.

3.3 Preliminary Considerations

3.3.1 The Conversion Requirement

The instantaneous resource can be measured at or close to a particular site by an appropriate measuring device, such as a wave recorder buoy, and is usually recorded as a discrete time series. The challenge is to convert the energy contained within the wave motion described by this time series into useful electrical energy.

An assessment of a favourable site is made usually by monitoring the wave climate over a considerable period to determine the variety and power contained within the various sea-states. It is instructive to review some basic properties of the resource from a hydrodynamic perspective and without impinging upon the detailed assessment of the resource presented in Chapter 4.

This challenge can be represented by considering two power spectra, each associated with the sites deemed favourable for energy extraction. Both spectra are shown in Fig. 3.2 and may be considered as being typical of the sites and containing at least a moderate level of power. The first is the "select spectrum" of Crabb (1980) and provides a model representative spectrum, based upon site measurements, from the South Uist site off the west coast of Scotland; the water depth is 42 *m* and the mean resource is estimated as 47.8 *kW/m*. The second spectrum is a measured spectrum from the island of Pico in the Azores, which was obtained as part of the development programme for the OWC built upon Pico and was supplied by Pontes and Oliveira (1992). The site is onshore with 8 *m* water depth, an estimated mean resource of 26.5 *kW/m* and the spectrum is considered to be reasonably energetic for the given site. These spectra possess similar peak values at almost the same frequency but the South Uist spectrum is broader and contains almost 80 % more power than the Pico one. A device designed to operate at either site must be capable of operating efficiently within the frequency range and power level.

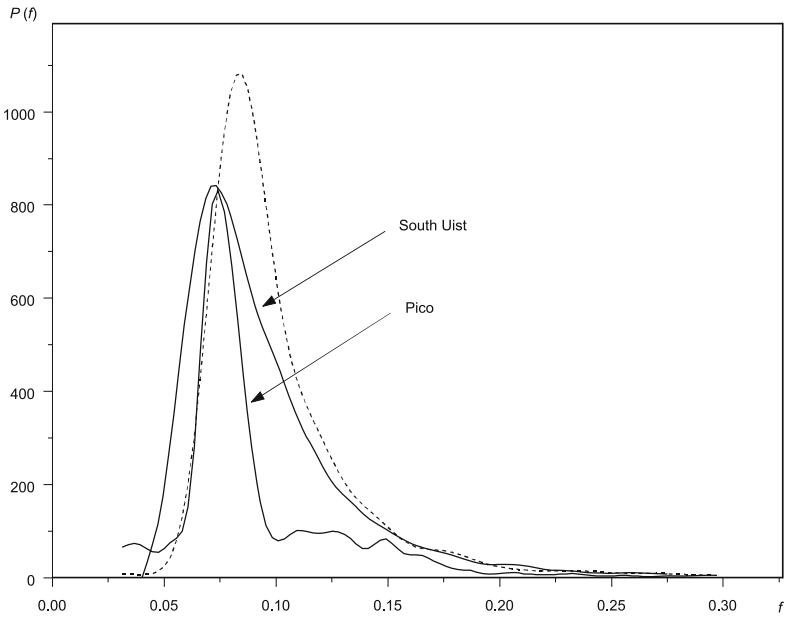

Fig. 3.2. Representative resource spectra for the Pico and South Uist sites, showing the power density $P(f)$ (in *kW/m/Hz*) against frequency f (in *Hz*). The solid lines show the site resource and the broken line corresponds to the offshore resource at Pico

Another Pico curve is also shown in Fig. 3.2 as a dotted line and this is the deepwater resource prior to reaching the shoreline, measured in 104 *m* of water and with a power level of 40.3 *kW/m*. A comparison of the deepwater and onshore resources shows that approximately one third of the power has been lost in the transition region between the two measuring sites, with the loss occurring in the shorter wavelengths. Another interesting feature is that the maximum value in the two spectra occurs at different frequencies, demonstrating the importance of establishing power levels at the installation site.

The power spectra in Fig. 3.2 provide good assessments of the resource and are obtained from surface elevation records that may or may not contain any measure of wave directionality. They provide a summary of individual sea-states but not of the water surface movements. A typical surface elevation associated with a particular spectrum can be obtained by extracting wave amplitude values at prescribed frequencies and then summing the contributions from the component frequencies, assigning a random phase difference to each frequency component. Such a surface elevation is shown for the Pico spectrum in Fig. 3.3. This represents the instantaneous resource and identifies the real challenge: to convert the time-varying incident power to useful electrical power or into some useful repository of power storage.

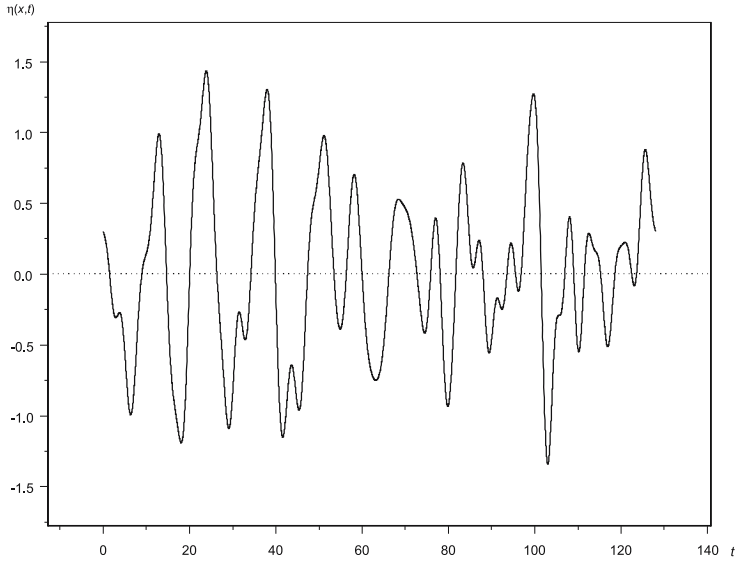

Fig. 3.3. A synthesised surface profile, showing the elevation η (in *m*) against time *t* (in *s*), corresponding to the Pico spectrum shown in Fig. 3.2

3.3.2 Modelling the Resource

To understand the requirement identified above, begin with a very simplified representation of the resource and employ elementary wave mechanics. Information on general water wave mechanics can be obtained from Dean and Dalrymple (1991) and more specialist applications to ocean waves from Goda (2000) and Tucker and Pitt (2001).

Choose co-ordinates (x, y, z) with *x,y* horizontal and *z* vertical, measured positive in an upward direction. The surface elevation in water of mean depth *h* is measured by a wave height recorder at a fixed point in space with horizontal co-ordinates (x_0, y_0) and the signal $z = \eta(x_0, y_0, t)$ may be continuous or discrete. As the measuring point is both fixed and general, the (x_0, y_0) part of the description can be neglected, provided it is recognised that a different signal will be found for each reference point. Thus the elevation may be considered just as $\eta(t)$ and is simply a continuous function of time that is known at any time *t*. Quantities requiring physical measurement typically employ *f*, the frequency in *Hz*, whereas it is often easier in modelling studies to employ ω, measured in *rad/s*. The two are related by $\omega = 2\pi f$ and both are used herein, as appropriate.

In a formal sense the signal at the fixed point can be regarded as being composed of a continuous spectrum of frequencies, each characterised by an amplitude density measure $a(\omega)$ and a phase function $\gamma(\omega)$, so that the surface can be characterised by

$$\eta(t) = \int_0^\infty a(\omega) \cos\left(\omega t - \gamma(\omega)\right) d\omega \,. \tag{3.1}$$

At any time $\eta(t)$ represents the integral under a curve in the frequency domain and so may also be represented approximately as the linear sum of an infinite number of frequency components,

$$\eta(t) = \sum_{m=0}^{\infty} a_m \cos\left(\omega_m t - \gamma_m\right) . \tag{3.2}$$

A comparison of Eqs. (3.1) and (3.2) suggests that the discrete amplitude a_m and continuous measure $a(\omega)$ are related by $a_m = a(\omega_m)d\omega$. Figure 3.3 was obtained from the Pico spectrum in Fig. 3.2 by employing the representation Eq. (3.2) with a finite rather than an infinite sum of components and with the phases chosen randomly.

If all of the amplitudes a_m in Eq. (3.2) are small in some sense, so that individual amplitude components are not bound to others within the series, then Eq. (3.2) can be regarded as a series of individual sinusoidal waves. The influence of each may be considered separately and then summed appropriately to obtain the influence of the complete spectrum. More specifically, each component will lie within the linear regime provided that $a_m k_m << 1$ and $a_m / h << 1$, where k_m is the magnitude of

the wavenumber vector and related to the wavelength by $k_m = 2\pi/\lambda_m$. If the problem cannot be treated in this manner then it is considered to be nonlinear.

The analysis above takes no account of directionality in the wave field and it is very rare for this to be unimportant. It may be of particular importance to a chosen site, as the bed topography may provide a focusing mechanism to enhance the resource. This can be included for linear wave components by interpreting Eq. (3.2) as

$$\eta(x,y,t) = \sum_{m=0}^{\infty} a_m \cos\left(k_m x \cos\beta_m + k_m y \sin\beta_m - \omega_m t + \psi_m\right) \tag{3.3}$$

evaluated at $x = x_0, y = y_0$ and $\gamma_m = -\left(k_m x_0 \cos\beta_m + k_m y_0 \sin\beta_m + \psi_m\right)$, with β_m being the angle between the direction of wave propagation and the *x*–axis. Thus Eq. (3.3) can be considered as being composed as a number of long-crested wave components propagating in arbitrary directions.

A further consequence of Eq. (3.3) is that it is sufficient to consider the influence of a single frequency component alone at an arbitrary angle of incidence within the linear wave regime, i.e., to assume that the surface elevation is given by

$$\eta(x,y,t) = a\cos\left(kx\cos\beta + ky\sin\beta - \omega t\right), \tag{3.4}$$

with the phase ψ_m taken to be zero. This does not mean that the time series approach is unimportant, and this is certainly not the case, but Eq. (3.4) confirms that many of the important properties of the device can be obtained by an analysis in the frequency domain.

For the regular incident wave represented by Eq. (3.4), the mean power (averaged over the wave period) per unit crest width is $\mathcal{P}_W = \frac{1}{2}\rho g a^2 c_g$, where c_g is the group velocity. If *P* is the mean power absorbed by the device, then the capture width $\mathcal{L}(\omega,\beta)$, identified in Section 3.2.1 as an important property, is defined by

$$\mathcal{L}(\omega,\beta) = \frac{\mathcal{P}}{\mathcal{P}_W}. \tag{3.5}$$

There will be no dependence upon β if the device is axisymmetric about a vertical axis.

The concept of a capture width is an appealing one, since it shows that the device captures an amount LP_W from the wavefront. This will not correspond to power taken from just a strip of width *L*, although the power extraction would be expected to occur primarily from the frontage area nearest to the device. However, it is not a non-dimensional measure of the optimal absorption characteristics of a device. The capture width possesses the dimension of length and this is because it employs the reference measure of mean power per unit width of wave crest. If *D* is a typical device dimension representing perhaps frontage to the incident waves, then an important measure for the device is *L/D*. It is clear that this should be as

large as possible and, from an intuitive perspective, values less than unity would be regarded as poor.

3.3.3 Survivability

For many WECs, the application of models provided by the small amplitude linear wave theories, within the context above, will be accurate for the vast majority of their operating times. However, such models will not suffice for force prediction or device behaviour when the WECs are exposed to very large wave-induced forces in extreme storm seas and the question of whether or not the device will survive such forces must be addressed. Wind loading may also be considerable for those devices that possess a substantial exposure above the water surface.

The potentially disastrous effects of storm seas provide part of the engineering and design challenge. It is fortunate that although it may not be possible to predict the wave-induced loading accurately, there is a solid base of work available from the offshore and maritime engineering industry that can be utilised as a starting point for WECs. However, it must be stressed that WECs introduce particular difficulties that have not been encountered previously with offshore structures. For example, the front wall of a shore-mounted OWC may appear to be rather like a breakwater and may be sloping or vertical, depending upon the designer's choice. If the breakwater survives then it serves its purpose and protects any features behind it. This is not the case with wave energy: the device must survive and must do so in such a way that the hydrodynamic behaviour of the OWC remains favourable for generative motion to take place within the OWC chamber as conditions demand. A number of innovative approaches have been proposed to enable survival of WECs, including submergence and intelligent control. Such considerations are beyond this contribution, except perhaps by way of introducing design constraints, and an interesting assessment of possibilities is given by Chaplin and Folley (1998).

It must be recognised that there is no requirement in storm seas to provide an efficient conversion chain from resource to grid: there is increased resource in such seas to require at most a moderate efficiency. However, survival is paramount and this defines the twin requirements of a WEC: very efficient conversion in small to moderate seas moving through to survival in storm seas. The importance of survivability is acknowledged to be of paramount importance but is not considered further in the conversion process.

3.4 The Hydrodynamics of Offshore Devices

It is important to recognise at the outset that the modelling of wave energy devices, although rooted in ship and offshore hydrodynamics, must necessarily possess a different viewpoint to that which exists in the parent fields. In offshore hydrodynamics, the purpose of a mathematical model is usually to determine the

wave loading on a fixed or floating structure of agreed design; in ship hydrodynamics it is the response of a specific ship design to certain sea conditions that is of interest. Neither approach is applicable in wave energy studies: the key to WEC modelling is performance. All other seemingly important quantities associated with device modelling, such as wave loading, are of secondary consideration even though they often appear as a result of, or are employed in, mathematical models of WECs. If a device cannot perform sufficiently well to absorb an acceptable level of power in small or moderate seas then other considerations are not investigated.

In the first instance, attention is restricted to those devices that are intended to operate in the offshore environment and particularly to floating structures. The principal class of devices excluded is the OWCs, of which the onshore category is more important presently. There are two reasons for separate consideration of these devices: an assessment of a fixed structure is not compatible with an analysis that places a strong emphasis upon a body movement and the power take-off mechanism of an OWC, involving aerodynamic - hydrodynamic coupling, also requires a specific treatment. A floating OWC will require a combination of both approaches to be employed; OWCs are considered separately in Section 3.7.

A general rigid body motion is composed of three translational modes of motion (surge, sway, heave) and three rotational modes of motion (roll, pitch and yaw) in the directions of and about the (x,y,z) coordinate axes. For convenience, consider the single tight-moored buoy shown in Fig. 3.4 with attention restricted to the heave or surge motions. This semi-submerged sphere is axisymmetric and can be taken to represent a generic device for the purposes of the present discussion. It can be described, in the terminology of Section 3.2, as a point absorber when it has a sufficiently small diameter, or as an attenuator or terminator if otherwise; it is classified as a second generation device although it was one of the first to be considered.

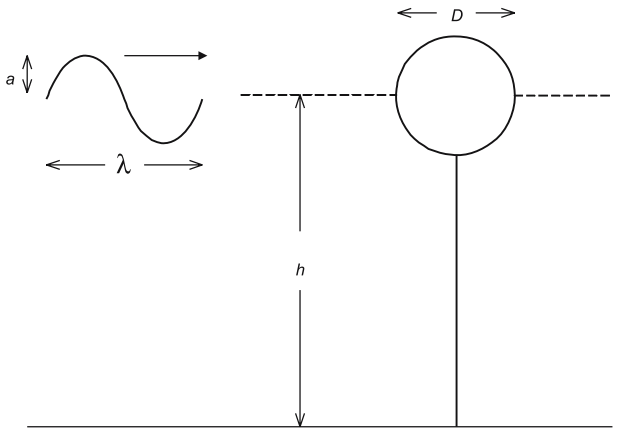

Fig. 3.4. Schematic of an axisymmetric heaving device

The modelling process is best described by considering a single translational mode in a long-crested incident wave field and the initial presentation follows that of Jefferys (1980). If m is the mass of the body and $X(t)$ represents its time-varying displacement, then the equation of motion of the body is given by

$$m\ddot{X} = F_T(t) + F_{ext}\left(X, \dot{X}, t\right), \tag{3.6}$$

where the total force $F_T(t)$ has components $F_f(t)$ and $F_{ext}(X, \dot{X}, t)$ denoting the wave/fluid induced forces and externally applied forces respectively acting in the direction of $X(t)$. The external forces can represent power take-off mechanisms and/or mooring constraints and the power take-off mechanism may be incorporated into the mooring system. Clearly the force will be dependent upon the type of mooring and the task that it is expected to perform. At this point, the formulation is exact.

3.4.1 Hydrodynamic Approximations

A regular incident wave field in water of depth h, as in Eq. (3.4), can be characterised by amplitude measure a, wavenumber k (or wavelength $\lambda = 2\pi/k$) and radian frequency ω. These will be related by a dispersion relation of the form $G(a, k, \omega, h) = 0$ and the character of the wave field can be described by the non-dimensional parameters ak and kh, associated with the wave-slope and water depth-to-wavelength ratio respectively. In water of intermediate depth or deep water, classified by $kh = \mathrm{O}(1)$ or $kh >> 1$, the nonlinearity is determined by the value of the wave slope ak. In shallow water, $kh << 1$, and the nonlinearity depends upon both ak and kh.

The structure can be characterised by an appropriate number of length scales dependent upon the body geometry. For the present general discussion, it is sufficient to permit just one length scale D and the diameter of the buoy in Fig. 3.4 is a good representative measure. The forces and pressures that represent the wave-structure interaction depend upon the appropriate non-dimensional ratios of the parameters that describe the individual components, so intuitively the dependency would be expected to be reflected by quantities such as kD, a/D, h/D and possibly some representation of viscosity. Combinations of these parameters are also important, with the Reynolds number R_e and Keulegan-Carpenter K_c being most prominent in the present discussion. The general definitions of these quantities can be adapted to the confines of linear wave theory, with K_c interpreted as the distance travelled by a particle relative to the length scale of the object, and taken for illustrative purposes as

$$R_e = \frac{aD\omega}{\nu}, \qquad K_c = \frac{2\pi}{\tanh kh}\frac{a}{D}. \tag{3.7}$$

Diffraction effects dominate when the flow remains laminar in the vicinity of the structure, viscous effects are negligible and no vortex shedding occurs. A con-

sequence is that if the incident waves are irrotational, then the flow within the vicinity of the body will also be irrotational and so a formulation in terms of a velocity potential may be employed. This is very enabling from both an analytical and numerical perspective.

The parameter kD (or $D/\lambda = kD/2\pi$) is often considered to be the measure of the importance of diffraction and Sarpkaya and Isaacson (1981) consider that diffraction should be included whenever $kD > 1.3$, equivalent to $D/\lambda > 0.2$. Based upon the allowable range of parameters before wave breaking, these authors consider that the resulting Keulegan-Carpenter number is bounded by $K_c < 0.07\,kD$ and will be at most 2.2 and usually less then unity. The requirement that $D/\lambda > 0.2$ for the diffraction regime to remain valid is important from a modelling perspective and easily tested. A full discussion is given by Sarpkaya and Isaacson (1981) and useful practical information can also be obtained from Faltinsen (1990) and Goda (2000). Within the present context, the number of frequencies in the incident wavetrain, as described by Eqs. (3.2) or (3.3), must be considered. It is assumed that the diffraction regime holds for each component in the spectrum and, for a body of given dimension, this imposes restrictions subsequently upon the frequency components that can be considered to lie within the diffraction regime.

It is usually assumed in preliminary models of WECs that the forces remain within the diffraction regime and that the importance of other known forces can be considered at a later stage. With attention confined to linear water wave theory in the diffraction regime, the fluid induced forces $F_f(t)$ can be approximated by the combination

$$F_f(t) = F_S(t) + F_R(t) + F_H(t), \tag{3.8}$$

where $F_S(t)$, $F_R(t)$ and $F_H(t)$ are the exciting, radiated and hydrostatic forces respectively. In this representation the exciting and radiated forces are associated with the response of the body to the incident wave motion and the hydrostatic component is independent of the waves; a complete discussion of this decomposition is given by Newman (1977). Each component will be considered separately.

With the incident wave given by Eq. (3.4), it often convenient in linear theory to employ a complex representation, so the surface elevation can be written as $\eta(x,y,t) = \mathrm{Re}\{a \exp i(kx\cos\beta + ky\sin\beta - \omega t)\}$. By analogy it is often assumed that the motion of the body in this single mode can be written as

$$X(t) = Re\{\xi e^{-i\omega t}\}, \tag{3.9}$$

where ξ is some unknown complex constant and which can only be determined via the solution of Eqs. (3.6) and (3.8). This complex form is a useful representation of $X(t)$. The magnitude of ξ corresponds to the magnitude of the oscillation and the phase is also important and may differ from that contained within the incident wave. The condition imposed by diffraction theory is that the quantity $|\xi|/a$ is at most of $O(1)$ and is consistent with the representation of the three terms that appear in Eq. (3.8). However, while the form Eq. (3.9) is clearly attractive, it

cannot be imposed without justification and the external force $F_{ext}(X,\dot{X},t)$ must be amenable to such a representation. The accompanying velocity field is

$$\dot{X}(t) = U(t) = Re\left\{\mathbb{U}\, e^{-i\omega t}\right\}, \quad \mathbb{U} = -i\omega\xi \tag{3.10}$$

and this is included here since it will be utilised at future points.

The view has been expressed previously that linear theory will be valid for most devices in most operating circumstances and that storm conditions will provide the principal exception. This is certainly the case for floating devices but a caveat needs to be imposed when nearshore or onshore WECs are considered. The nearshore wave climate often lies within the shallow water regime and the demands placed by the condition that the *Stokes* (or *Ursell*) parameter $(ak)/(kh)^3$ is $<<1$ for the applicability of linear theory is severely restrictive. This does not mean that nearshore WECSs cannot be considered using linear theory, it is more that linear theory may not provide a sufficiently accurate working environment for a substantial period of operational time.

The *Exciting* (or *Scattering*) *Force* $F_S(t)$ is the force that the body would experience if it were held fixed in its mean position and, in keeping with Eq. (3.9), is usually written as

$$F_S(t) = Re\left\{\mathbb{X}\, e^{-i\omega t}\right\}, \tag{3.11}$$

for some complex constant $\mathbb{X}$. Some texts employ $\mathbb{X}_s$ instead of $\mathbb{X}$ but there is no inconsistency or confusion in using the simpler form here. This quantity can be considered as being composed of two parts,

$$\mathbb{X} = \mathbb{X}_{inc} + \mathbb{X}_{diff}, \tag{3.12}$$

corresponding to contributions from the incident and diffracted waves respectively. The quantity $\mathbb{X}_{inc}$ is usually straightforward to obtain and corresponds to integrating the known pressure due to the incident waves over the wetted body surface. In contrast, determination of the second term $\mathbb{X}_{diff}$ is often a difficult task and this quantity can only be calculated when the pressure field over the whole wetted surface has been determined. Analytical or semi-analytical solutions are rare and restricted to very simple geometries; solutions must be sought numerically in most cases of practical interest and these utilise industry standard codes. The numerical methods employed have been developed in the fields of naval hydrodynamics and offshore engineering and are described in Chapter 5, providing another good example of the benefit of retaining a link with a cognate technology. A good summary of the available mathematical techniques for problems of this type is given by Linton and McIver (2001). If $\left|\mathbb{X}_{diff}\right| << \left|\mathbb{X}_{inc}\right|$ then the diffracted component can be neglected and the scattered force is represented by the contribution from the incident waves alone. This is known as the *Froude-Krylov Approximation* and is clearly useful when circumstances permit.

The *Radiation Force* $F_R(t)$ corresponds to the force experienced by the body due to its own oscillatory movement in the absence of an incident wave field and is proportional to the amplitude $|\xi|$ of the displacement in the linear theory. The standard practice is to regard the force as being composed of two components: one in phase with the body acceleration and the other in phase with the body velocity, i.e.

$$F_R(t) = -\left\{ A(\omega)\ddot{X} + B(\omega)\dot{X} \right\}, \tag{3.13}$$

where $A(\omega)$ and $B(\omega)$ are known as the added mass and damping coefficients respectively. In keeping with Eq. (3.9) and Eq. (3.11), write Eq. (3.13) as

$$F_R(t) = Re\left\{ \mathbb{F}_R e^{-i\omega t} \right\}, \quad \mathbb{F}_R = \left[\omega^2 A(\omega) + i\omega B(\omega) \right] \xi . \tag{3.14}$$

Falnes (2002), and in earlier papers, has made extensive use of analogies with applications in other oscillatory systems. Following this approach, the radiation force is then written

$$\mathbb{F}_R = -\overline{Z}(\omega)\mathbb{U} \qquad Z(\omega) = B(\omega) + i\omega A(\omega), \tag{3.15}$$

where the complex quantity $Z(\omega)$ is termed the *Impedance* or the *Radiation Impedance*, the overbar denotes the complex conjugate and $\mathbb{U}$ has been given in Eq. (3.10). Whether $Z(\omega)$ or $\overline{Z}(\omega)$ appears in Eq. (3.15) depends upon the form of the time dependency employed in Eqs. (3.9) and (3.11); the conjugate is required if the time dependency is taken to be $e^{-i\omega t}$ but not if $e^{i\omega t}$ is used. Although the latter may appear more appropriate in standard oscillator applications, the former is employed here to retain the same time dependency as that of the incoming wave field, given immediately prior to Eq. (3.9).

As with the diffracted force $\mathbb{X}_{diff}$ in Eq. (3.12), the determination of $A(\omega)$ and $B(\omega)$ is a task that must be accomplished numerically in most cases of practical interest, with the available mathematical approaches being summarised by Linton and McIver (2001). Fortunately, as in the numerical determination of $\mathbb{X}_{diff}$, $A(\omega)$ and $B(\omega)$ can be obtained employing the same numerical algorithm so that some efficiency is possible in the solution of this difficult numerical problem.

The *Hydrostatic Force* $F_H(t)$ is the buoyancy force on the device and given by

$$F_H(t) = -CX(t) = -Re\left\{ C\xi e^{-i\omega t} \right\}, \tag{3.16}$$

where C is the buoyancy coefficient. If the body is in a position of equilibrium in the absence of waves, then this is only non-zero for the heave (vertical) mode of motion and for the roll and yaw rotational modes of a floating body.

3.4.2 The Equation of Motion

Return to the exact equation of motion Eq. (3.6) and employ the approximations consistent with the assumptions that the incident waves are regular and linear, that the forces remain within the diffraction regime and the magnitude of the body motion is comparable to the incident wave amplitude. Combining Eqs. (3.6) and (3.8), for the wave-fluid interaction forces then gives the equation of motion $m\ddot{X} = F_S(t) + F_R(t) + F_H(t) + F_{ext}(X, \dot{X}, t)$. Introducing the appropriate forms from Eqs. (3.11) – (3.16) for the force representations gives

$$\left(m + A\right)\ddot{X} + B\dot{X} + CX = Re\left\{\mathbb{X}\, e^{-i\omega t}\right\} + F_{ext}(X, \dot{X}, t)\,, \tag{3.17}$$

which, via Eq. (3.9), can also be written as

$$Re\left\{\left[-\omega^2\left(m + A\right) - i\omega B + C\right]\xi e^{-i\omega t}\right\} = Re\left\{\mathbb{X}\, e^{-i\omega t}\right\} + F_{ext}(X, \dot{X}, t)\,. \tag{3.18}$$

At first glance Eqs. (3.17) and (3.18) may appear to describe a standard harmonic oscillator but this is not the case, since the equation can only be consistent if F_{ext} has the same time dependency as those terms based upon the incident wavetrain. Jeffreys (1980) states that it is not even a differential equation in the standard sense! The form of $F_{ext}(X, \dot{X}, t)$ is crucial to further progress and this has already been identified as an important factor in enabling Eq. (3.9) and upon which Eq. (3.18) is based. A simple linear damper model is often chosen to represent the power take-off mechanism but this may not always be a realistic approximation. Mooring forces should also be included whenever present and a taut mooring can provide a significant influence upon the device motions.

An extension to the impedance approach of Eqs. (3.14) and (3.15) is also possible. With $Z_T(\omega)$ defined by

$$Z_T\left(\omega\right) = Z\left(\omega\right) + i\left(\omega m - C/\omega^2\right) = B(\omega) + i\omega\left(A(\omega) + m - C/\omega^2\right), \tag{3.19}$$

Eq. (3.18) becomes

$$Re\left\{\overline{Z_T}\left(\omega\right)\mathbb{U}\, e^{-i\omega t}\right\} = Re\left\{\mathbb{X}\, e^{-i\omega t}\right\} + F_{ext}(X, \dot{X}, t)\,. \tag{3.20}$$

the usefulness of this form is dependent upon the structure of F_{ext}, upon its time dependence in particular and will be considered in Section 3.6.

The derivation above has assumed, for simplicity, that the body undertakes a single translational mode of motion. As stated previously, a general rigid body motion will be composed of three translational modes and three rotational modes. These can be accommodated in the present framework by extending $X(t)$, presently representing a single translational mode, to the column vector $\boldsymbol{X} = \left\{X_j, j = 1,2,...,6\right\}$ and where the first three components of $\boldsymbol{X}$ represent the translational modes and the second three are the rotational modes. In a similar manner, quantities appearing as forces are also six-component column vectors and

are associated with both forces and moments in the same manner as $\boldsymbol{X}$. The corresponding extension to Eq. (3.17) is

$$\sum_{j=1}^{6}\left[\left(m_{kj}+A_{kj}\right)\ddot{X}_j+B_{kj}\dot{X}_j+C_{kj}X_j\right]=Re\left\{\left(\mathcal{X}\right)_k e^{-i\omega t}\right\}+\left(F_{\boldsymbol{ext}}(X,\dot{X},t)\right)_k, \quad (3.21)$$

where $k=1,2,\ldots,6$. A complete description for sinusoidal motion is provided by Newman (1977). The added mass and damping matrices are symmetric and again usually require numerical determination, via the codes described earlier.

While the form Eq. (3.6) is exact, all of the ensuing discussion assumes that the waves are monochromatic and linear, that the wave loading is within the diffraction regime and the external force is of an amenable form. Suppose that the latter two of the three conditions remain valid but the waves are no longer of a single frequency. In principle it is possible to adopt the approach of Eqs. (3.2) and (3.3) and consider all frequency components independently, with the final result requiring a careful combination of all components and their phases. It is more usual to employ the time-dependent form of the equation of motion and the changes moving from regular to irregular wave fields are examined.

Equation (3.18) was obtained by employing the decomposition Eq. (3.8) and then approximating each of the component terms for a regular wave motion. When an irregular wave field is present, only the hydrostatic component $F_H(t)$ in Eq. (3.16) remains unchanged. The exciting force $F_S(t)$ cannot be modelled in a harmonic manner and must be included in a general form and the radiation force $F_R(t)$ is modelled via the derivation given by Cummins (1962). For a single mode of motion the equation is

$$\left(m+A_\infty\right)\ddot{X}+\int_0^t K(t-\tau)\,\dot{X}(\tau)\,d\tau+CX=F_s(t)+F_{ext}(X,\dot{X},t), \quad (3.22)$$

where A_∞ is a constant related to the added mass and $K(t-\tau)$ is an impulse response function related to the radiation damping. A full review of floating body hydrodynamics within the diffraction regime is given by Wehausen (1971) and the applicability to WEC modelling is described in Jefferys (1980).

3.5 Optimal Hydrodynamic Performance

Much of the original work on the extraction of power from waves drew heavily upon the expertise of practitioners in marine hydrodynamics and particularly upon those associated with mathematical modelling in the offshore environment. Newcomers to the field were able to draw upon a considerable resource of material that could be adapted readily to their own uses. It is not possible to attribute all of the many contributions made during this classical period of hydrodynamic device performance and more complete accounts are given in a major paper and review by Evans (1980, 1981a) and in the text of Falnes (2002), these being two of the most prominent contributors. The notation adopted here tends to follow that of Evans.

The instantaneous power associated with a general force $F(t)$, acting on a body in a single translational mode of motion described by the displacement $X(t)$, is the instantaneous rate of work given by

$$P(t) = F(t)\dot{X}(t) = F(t)U(t)\,. \tag{3.23}$$

The mean power absorbed per wave cycle P_M, or whatever time interval is specified, is

$$\mathcal{P}_M = \left\langle F(t)\dot{X}(t)\right\rangle = \left\langle F(t)U(t)\right\rangle, \tag{3.24}$$

where $\langle\ \rangle$ denotes the time average over the specified period and $U(t) = \dot{X}(t)$ has been introduced from Eq. (3.10), as it is sometimes more convenient to work with velocity components directly rather than with derivatives of the displacement.

Now assume the waves are monochromatic, linear and that the forces are within the diffraction regime. The mean power generated by the fluid (hydrodynamic) forces, using Eqs. (3.8) and (3.24), is

$$\mathcal{P}_{Mf} = \left\langle F_f(t)U(t)\right\rangle = \left\langle \left[F_S(t) + F_R(t) + F_H(t)\right]U(t)\right\rangle,$$

with the individual forces given in Eqs. (3.11) – (3.16) and the velocity by Eq. (3.10). It is clear that the averaging will produce non-zero contributions only from those force components in phase with the velocity $U(t)$ and so neither the added mass nor the hydrostatic force will contribute.

This concept is readily extended to include all possible modes of motion in a manner similar to which the equation of motion in a single mode Eq. (3.17) was extended to Eq. (3.21) for all modes. It can be shown that the mean hydrodynamic power generated by a body in general motion, i.e. all six modes of motion, is

$$\mathcal{P}_{Mf} = \frac{1}{2}Re\left\{\mathbb{X}^*\mathbb{U}\right\} - \frac{1}{2}\mathbb{U}^*B\mathbb{U}\,, \tag{3.25}$$

where the superscript * denotes the complex conjugate transpose when applied to square matrices or column vectors. The expression can also be written as

$$\mathcal{P}_{Mf} = \frac{1}{8}\mathbb{X}^*\boldsymbol{B}^{-1}\mathbb{X} - \frac{1}{2}\left(\mathbb{U} - \frac{1}{2}\boldsymbol{B}^{-1}\mathbb{X}\right)^*\boldsymbol{B}\left(\mathbb{U} - \frac{1}{2}\boldsymbol{B}^{-1}\mathbb{X}\right) \tag{3.26}$$

under the assumption that $\boldsymbol{B}^{-1}$ exists and which holds for most circumstances of interest. Both terms in this equation are always positive; the first is fixed for a particular geometry whereas the second is not, since $\mathbb{U}$ can be controlled.

Thus the maximum value of $\mathcal{P}_{Mf}$ is given by the first term and occurs when the second takes its minimum value, which is zero, to give

$$\mathcal{P}_{opt} = \frac{1}{8}\mathbb{X}^*\boldsymbol{B}^{-1}\mathbb{X} \tag{3.27}$$

and this occurs when

$$\mathbb{U} = -i\omega\boldsymbol{\xi} = \frac{1}{2}\boldsymbol{B}^{-1}\mathbb{X} \quad \Rightarrow \quad \boldsymbol{\xi} = \frac{i}{2\omega}\boldsymbol{B}^{-1}\mathbb{X}\,. \tag{3.28}$$

Thus P_{opt} depends upon both the body geometry (via $\boldsymbol{B}$) and the interaction between the incident waves and the body (via $\mathbb{X}$). In addition Eq. (3.28) identifies clearly the requisite body motion in both amplitude and phase for maximum power absorption. As $\boldsymbol{B}$ is real by construction, the required phase of the velocity is that of the exciting force. The notation P_{opt} is used to denote the maximum rather than P_{max} as the quantity represents the optimal value, i.e. the best that can be achieved and not diminished by restrictions introduced by the power take-off system or other physical constraints.

The capture width $L(\omega,\beta)$ was introduced previously as a suitable measure of power absorption and given in Eq. (3.5). Newman (1976) has shown the rather surprising result that it is possible to relate the damping matrix $\boldsymbol{B}$ to the exciting force vector $\mathbb{X}$, so that Eqs. (3.5)and (3.27) can be combined to give

$$\mathcal{L}_{\text{opt}}(\omega,\beta) \;=\; \frac{\lambda}{2\pi}\mathbb{X}^{*}\boldsymbol{W}^{-1}\mathbb{X} \qquad (\boldsymbol{W})_{mn} = \frac{1}{2\pi}\int_0^{2\pi}\mathbb{X}_m(\theta)\,\overline{\mathbb{X}_n(\theta)}\,d\theta\,, \tag{3.29}$$

where the overbar denotes the complex conjugate. Thus the optimal capture width and the body motion required to achieve maximum capture depend upon the interaction between the incident waves and the body when held in a fixed position. This is a generic and rather remarkable result!

The form of Eq. (3.29) becomes much simpler when the device is restricted to a single mode of motion and thus Eqs. (3.27) and (3.28) become

$$\mathcal{P}_{opt} = \frac{\left|\mathbb{X}(\beta)\right|^2}{8B} \quad \text{when } \mathbb{U} = \frac{\mathbb{X}}{2B}\,. \tag{3.30}$$

Newman (1976) has also shown that the exciting force $\mathbb{X}$ in this case can be related to the angular dependence $\mathbb{A}(\beta)$ of the radiated wave field. Thus Eq. (3.29) may be replaced by either of the following alternative versions,

$$\mathcal{L}_{opt}(\omega,\beta) \;=\; \lambda\frac{\left|\mathbb{X}(\beta)\right|^2}{\int_0^{2\pi}\left|\mathbb{X}(\theta)\right|^2 d\theta} \;=\; \lambda\frac{\left|\mathbb{A}(\beta)\right|^2}{\int_0^{2\pi}\left|\mathbb{A}(\theta)\right|^2 d\theta} \tag{3.31}$$

and the choice of application depends upon which of $\mathbb{X}(\theta)$ and $\mathbb{A}(\theta)$ is easier to determine.

3.5.1 A Single Axisymmetric Device

The exciting force $\mathbb{X}$ and angular variation $\mathbb{A}$ will be independent of the incident direction θ. For an axisymmetric device operating in heave Eq. (3.31) reduces to the simple form

$$\mathcal{L}_{opt}(\omega,\beta) = \frac{\lambda}{2\pi} \tag{3.32}$$

for a heaving buoy. This benchmark result was derived independently, and in slightly differing ways, by a number of contributors including Budal and Falnes (1975), Evans (1976), Mei (1976) and Newman (1976).

Writing the body motion as $X(t) = Re\left\{a\mathbb{D}e^{-i\omega t}\right\}$ enables $\mathbb{D}$ to be determined via Eqs. (3.9) and (3.28) as

$$\mathbb{D} = \frac{i}{2a\omega}\frac{\mathbb{X}}{B} = \frac{4iP_w}{ak\omega\overline{\mathbb{X}}} \tag{3.33}$$

and $|\mathbb{D}|$ is known is the *Displacement Amplitude* or *Amplitude Ratio*, representing the ratio of the body displacement to the wave amplitude at optimal power take-off. The linear theory and diffraction regime permit this to be at most of O(1) but this measure may not provide substantial information on the physical displacement and the acceptability of the predicted measure must be determined from practical considerations. If the amplitude displacement induces excessively large motions in the power take-off mechanism, it may violate a physical constraint upon the possible motion and this is sometimes referred to as the end-stop problem. A ratio based upon the incident wave amplitude, such as $|\mathbb{D}|$, is a useful quantity from a mathematical modelling perspective but the physical value determining the end-stop will depend upon the device and not the non-dimensional amplitude.

The importance of Eqs. (3.32) and (3.33) is clear: the maximum power that an axisymmetric buoy can extract in heave is given by $\lambda/2\pi$ irrespective of the scale of the device. However, as a general rule, the magnitude of $\mathbb{X}$ will increase with body diameter and a larger body will possess a smaller displacement amplitude. Thus decreasingly smaller buoys will need to perform increasingly large oscillations and this may violate physical and modelling constraints. An assessment can be made of the applicability of the diffraction theory in such cases, using the criterion that diffraction effects become important whenever the non-dimensional parameter $kD > 1.3$ ($D/\lambda > 0.2$) and where D can be taken to be the diameter of the device. As D becomes smaller the point absorber approximation of determining $\mathbb{X}$ from $\mathbb{X}_{inc}$ alone, as discussed in Eq. (3.12), becomes more valid. However, the accuracy of the model may be reduced in such cases, since the decrease in diffractive effects is accompanied by an increase in the importance of viscosity.

There is also a further consideration. If the non-dimensional optimal capture width $\hat{\mathcal{L}}_{opt}$ is defined to be the ratio of the capture width to the width of the device, then from Eq. (3.33),

$$\hat{\mathcal{L}}_{opt}(\omega,\beta) = \frac{\lambda}{2\pi D} = \frac{\lambda}{4\pi R}, \tag{3.34}$$

where D and R are the diameter and radius of the device, respectively. This may be regarded as a measure of the structural efficiency, since it increases with decreasing radius and shows, with Eq. (3.32), that a balance must be sought between acceptable cost and realistic displacement amplitudes.

For a horizontal motion, Newman (1962) has shown that $\mathcal{A}(\theta)$ is proportional to $\cos\theta$ and so Eq. (3.31) provides the analogous result of

$$\mathcal{L}_{opt}(\omega,\beta) = \frac{\lambda}{\pi}\cos^2\beta. \tag{3.35}$$

This is maximum when $\beta = 0$ or π, giving an optimal capture width of λ/π when the body motion is in alignment with the waves. Thus the maximum power absorption for a horizontal mode is twice that of a heave mode. The heave and surge point absorber results in Eqs. (3.32) and (35) are important results but their significance does not just lie with point absorbers, they provide a benchmark for the absorption properties of any device being compared with a point absorber.

3.5.2 Constrained Motion

A drawback of the optimal result in Eq. (3.28) is that it may only be achievable if large displacement amplitudes, such as that given by Eq. (3.32) for a single mode, are permissible. This will not usually be the case and the end-stop problem will impose a physical constraint in addition to considerations associated with ensuring the validity of modelling within the diffraction regime. For a body undertaking a single mode of motion, Evans (1981b) imposed a constraint equivalent to one upon the non-dimensional displacement amplitude of the form

$$|\mathbb{D}| \le \varepsilon. \tag{3.36}$$

The corresponding maximum power absorbed $\mathcal{P}^c_{opt}$, obtained by constrained optimisation, can be written as $\mathcal{P}^c_{opt}(\beta) = \frac{|\mathbb{X}(\beta)|^2}{8B}\left\{1-(1-\delta)^2 H(1-\delta)\right\}$, where $\delta = \varepsilon/|\mathbb{D}|$ is the ratio of the maximum permissible amplitude imposed by the constraint and the displacement at optimal performance. The function $H(x)$ is the Heaviside step function, defined to take the values of zero and one when the argument is negative or positive respectively. Thus the constraint becomes active whenever $\delta < 1$ and there is an accompanying reduction in the maximum power.

As the optimal power P_{opt} is given in Eq. (3.30), define the non-dimensional constrained power absorption ratio by

$$\hat{\mathcal{P}}_{opt}^{c} = \frac{\mathcal{P}_{opt}^{c}(\beta)}{\mathcal{P}_{opt}(\beta)} = 1-(1-\delta)^{2} H(1-\delta) \tag{3.37}$$

and this shows the influence of the constraint explicitly. The relationship holds universally for a single mode of constrained motion and is shown in Fig. 3.5.

If $\hat{\mathcal{P}}_{opt}^{c}$ or the constrained capture width $\mathcal{P}_{opt}^{c}(\beta)$ is sought for a particular device, it can be obtained from Eq. (3.37) but evaluation may be a far from trivial task. The constraint parameter δ depends upon the exciting force and the damping, as does the optimal power P_{opt}; these two quantities need to be calculated for particular devices and evaluation may be analytic or numerical, more often the latter. Evans presents the constrained curves for the point absorber in Fig. 3.4 and also for other representative devices of generic interest.

The original constraint derived by Evans is more general than the one presented above for a single body in a single mode of motion and is a global constraint derived for a number of bodies oscillating independently, each capable of absorbing energy from the incident wave field. It is imposed via the sum of the squares of the individual velocities. Pizer (1993) has extended this approach to a global weighted constraint for a single body moving in more than one independent mode, which permits an interesting assessment to be made of the potential power absorption in multi-mode power take-off. However, it must be noted that the analytical

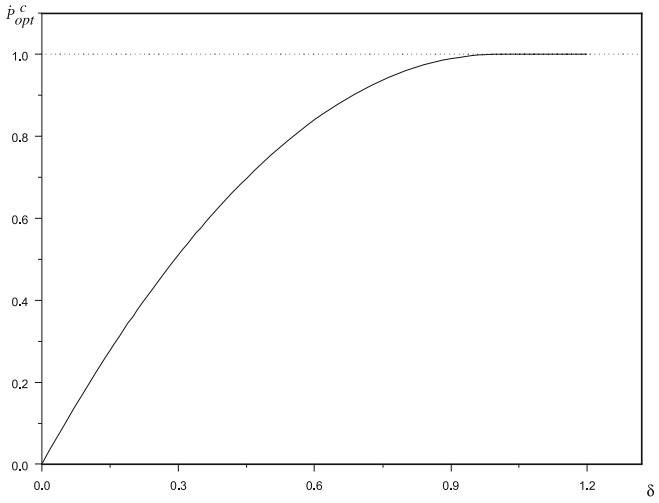

Fig. 3.5. Variation of the non-dimensional capture width $\hat{\mathcal{P}}_{opt}^{c}$ with constraint parameter δ

approach cannot be employed to enforce individual constraints, either on a particular body or mode of motion, and these need to be imposed numerically.

3.5.3 Arrays of Devices

Many devices are anticipated as operating in an array and the behaviour of the array members may be controlled for best individual or best array performance. Indeed when a new device is proposed, initial publicity usually contains an "artist's impression" of an array (or "farm") of the devices operating in long-crested seas. The array typically has many rows and while this may appear impressive initially, an analysis of array performance will most likely tell another story.

The fundamental modelling on arrays of wave energy devices was presented independently by Evans (1979) and Falnes (1980). Most work has assumed that the devices will be axisymmetric and this limitation will be enforced here. For a system of N bodies constrained to operate in just the heave mode of motion, the maximum power absorption is given by a form of Eq. (3.26), $\mathcal{P}_{opt} = \frac{1}{8}\mathbb{X}^* \boldsymbol{B}^{-1}\mathbb{X}$. The complex exciting force $\mathbb{X}$ and damping $\boldsymbol{B}$ now describe the interaction between the N members of the array and are an N-dimensional column vector and a square $N\times N$ matrix respectively. The corresponding capture width can be written as

$$\mathcal{L}_{opt}(\omega,\beta) = \frac{\lambda}{2\pi} N\, q(\omega,\beta)\,. \tag{3.38}$$

It is known from Eq. (3.32) that $\lambda/2\pi$ is the capture width of a single device in heave and hence q represents the ratio of the power absorbed by the array relative to that which would be absorbed by the N array members acting independently in heave and in isolation. Thus q is dependent upon the parameters that define the formation of the array and the geometry of its members, the frequency of the incident wave field and the orientation of the array relative to the incoming wave field. The value $q=1$ indicates no net influence of the array formation. *Constructive Interference* occurs when the total power output of the array exceeds that of N individual devices and *Destructive Interference* occurs when there is a net loss of generated power; these correspond to $q>1$ and $q<1$ respectively. For an array of bodies of given dimension the aim is to obtain $q\geq 1$ by an appropriate choice of power take-off and spacing parameters.

The concept has clear analogies with the theory of radio antennae and the prediction of the interactions, via the scattered wave fields, requires the determination of $\mathbb{X}$ and $\boldsymbol{B}$. This is a difficult task unless some simplifying approximations are made. One of the initial investigations was by Thomas and Evans (1981), who studied single and double row arrays, with each row composed of five equally-spaced members; other unreported studies by the same authors included two, three

and ten members in the array. Two body geometries were employed: the semi-submerged sphere of Fig. 3.4 and a thin ship, chosen as it possessed strong geometrical bias. Figure 3.6 below is taken from Thomas and Evans (1981) and shows the variation of q-factor with the non-dimensional measure $kd = 2\pi d/\lambda$, d being the spacing between members, for a row of five semi-submerged spheres for head, beam and $\pi/4$ incident seas. It is presented here for illustrative rather than definitive purposes, since array analysis contains many parameter combinations and conclusions cannot be drawn readily from a single figure.

One of the key features of this figure is the confirmation that regions of both constructive and destructive interference exist and that such regions cannot be avoided for the parametrical settings of the study. The performance is generally better in beam seas, though not always, consistent with the intuitive concept of greater frontage to the waves providing a greater opportunity for absorption. Although not shown here, the device members did not work equally hard, although there was symmetry about the central member in all cases corresponding to no sense of attenuation. Global and individual constraints were imposed numerically, as an extension of Eqs. (3.37) and (3.38); it was found that limiting the displacements to two or three times the incident wave amplitude was not severely restric-

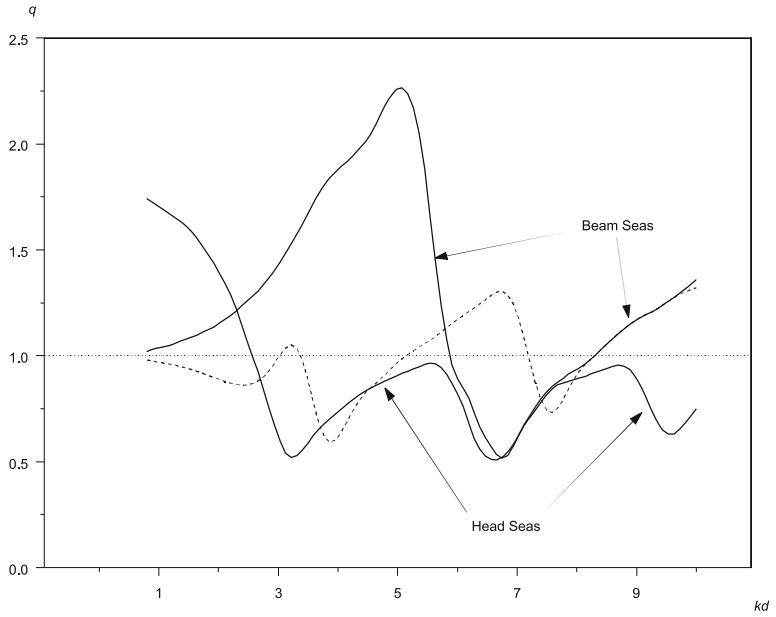

Fig. 3.6. Variation of the q-factor with the non-dimensional spacing parameter kd, for a uniformly-spaced linear array of five semi-submerged spheres and incident waves corresponding to beam and head seas (solid lines) and at $\pi/4$ (broken line). The dashed line $q = 1$ is equivalent to no interaction between array members

tive. The constructive interference decreased in magnitude but the regions of destructive interference were not significantly affected.

Later studies by McIver (1994), Mavrakos and McIver (1997) and Justino and Clément (2003) have also concentrated upon one or more linear arrays of small devices of the point absorber type, taut-moored and operating in heave. Variants on the earlier work include the influence of unequal spacing, constrained motions, full diffraction modelling and simultaneous consideration of all three translational modes of motion. However, the general features of array performance described by Thomas and Evans (1981) remain unchanged: regions of constructive and destructive interference occur generally and gains will be accompanied by losses. This remains a topic for much further work and perhaps justly so, as the alternative classification strategy of Section 3.2.3 places arrays of small devices in the third generation category.

3.5.4 Elongated Bodies

The general theory presented in the preceding sections, with the exception of the above discussion on arrays, is targeted at a single body capable of extracting power from the six independent modes of motion. However, the generic attenuator shown in Fig. 3.1 was conceived originally as being capable of extracting power as the wave moved along its length; it is also associated with low mooring forces, in contrast to those for a device of terminator type. The power take-off mechanism was not specified in the general case, although this will affect the chosen mode. Possibilities include articulated sections and a constant internal volume employing a pneumatic principle. Such devices are intended to work only in head seas and this restriction is enforced here by considering the case $\beta = 0$ only.

The seminal work is by Newman (1979), who considered a compliant body undertaking vertical displacements along its length. As a generalisation of the solid body modes of Eq. (3.9), the compliant motion is represented as a combination of possible independent modes $z = Re\left\{\zeta(x)\, e^{-i\omega t}\right\}, \zeta(x) = a\sum_j \upsilon_j \mathbb{Z}_j(x)$, with $\mathbb{Z}_j(x)$ denoting the j-th body mode, which is to be specified, and υ_j denotes the unknown complex amplitude associated with the mode. By consideration of individual modes it was shown that the maximum capture width associated with the general j-th mode is given by

$$\mathcal{L}_{opt,j}(\omega) = \lambda \frac{\left|H_j(\beta)\right|^2}{\int_0^{2\pi} \left|H_j(\theta)\right|^2 d\theta} \tag{3.39}$$

where $H_j(\theta)$ denotes the Kochin function for the j-th mode and which is related to the radiated wave field function $\mathcal{A}(\theta)$ in Eq. (3.31). Both Eqs. (3.32) and (3.35) can be deduced from Eq. (3.39) using similar arguments as before.

Slender body theory is valid in head seas when the beam and draft of the body are much less than its length. With this restriction placed upon the body geometry, Newman considers polynomial, trigonometric and piecewise linear modes and reaches some far-reaching conclusions, of which the two most prominent concern a hinged device and the optimal body length. For a hinged device, it is deemed sufficient from a practical viewpoint to have a single hinge and this should be placed away from the ends. If the most energetic waves are in the wavelength range of 100–200 *m*, then the optimal length of a compliant device appears to be of the order of the target incident wavelength.

Evans and Thomas (1981) considered a different attenuating device, the Lancaster Flexible Bag. This was described by Chaplin and French (1980) and operates by permitting a variable width along its length and subject to a global volume constraint. In addition, the device possesses small beam and draft relative to its length and is constructed to behave symmetrically about its vertical length-wise centre-plane. In contrast to Eq. (3.39), which described vertical motions, a width function $w(x) = Re\left\{\zeta(x)e^{-i\omega t}\right\}$ may be employed to describe the body motion. By considering $w(x)$ to be composed of a number of piecewise constant boxes and employing the Froude-Krylov approximation, a model was constructed very similar to the array structures of the previous section and included the capability of applying both global and (unpublished) individual constraints. Greater accuracy was achieved by increasing the number of boxes and a reasonable estimate of the maximum capture length would be half the body length. Local constraints can reduce this value and there is no attenuation along the bag, so that the rear portion must work as hard as the front portion.

The other geometry of interest in this category is the Pelamis, which is classified as an attenuator and belongs to the third generation category; the device team appears to prefer the descriptor *Line Absorber*. In its present form its dimensions are 140 *m* in length with a diameter of 3.5 *m*, so the slender body approximation is valid from a modelling perspective. The device body possesses four segments, with the three interlinking flexible joints containing the power take-off system. Those advantages attributed to elongated devices, such as low mooring and good survivability, have been confirmed by an extensive modelling and testing programme. However, there is one major difference between the Pelamis and the generic structures discussed above. This concerns the mode of motion: the Pelamis permits horizontal hinging about its joints, so that there need not be a vertical centreplane of symmetry along the length of the device when it is operation. It is suggested that the capture width of the device, extracting power in more than one mode of motion, is in the vicinity of $\lambda/2$ for typical sea conditions. Recent work on the device is contained in Pizer et al. (2005) and earlier work may be tracked from the references therein.

3.6 Control and Design

The results presented in the previous section are optimal results from a hydrodynamic analysis and there is no guarantee or expectation that such levels of power absorption can be achieved in practice. This is not to decry their usefulness and they provide both upper bounds and a filtering process that can be used to good effect. What is missing is this approach is a link between the final output and the input to the process. To establish this link it is useful to concentrate upon the processes of how to design a device and control the output from a hydrodynamic modelling perspective.

The earliest control strategies were devised to ensure that point absorbers operating in regular seas could maximise the converted power. This process required the phase and amplitude of the oscillation to be chosen to ensure optimal performance. However, the phase and the amplitude can be varied independently and so the two distinct aspects became known as *Phase Control* and *Amplitude Control*. More recently the terminology has been simplified to *Control*, as the field of application has widened and includes sub-optimal strategies. *Optimal Control* is sometimes used to refer to those cases where the aim is to convert the optimal amount of power. The maximum power absorption based upon hydrodynamic considerations alone corresponds to optimal control, as it determines both the phase and amplitude of the desired motion. This is seen clearly for a single body in multi-mode operation from Eqs. (3.27) and (3.28) and for a single mode from Eq. (3.30), where the optimal result is obtained by forcing both the amplitude and phase to take particular values.

It is clear from the equations of motion in Eqs. (3.17) and (3.22) for regular or irregular wave motion that any device can be considered as a mechanical system with two sets of parameters. For convenience these parameters are termed *Geometrical Parameters* and *Control Parameters*, though there is no accepted usage of these terms. *Geometrical Parameters* define the structure of the device and cannot be changed once the device has been built; these are represented here by the vector $\boldsymbol{G}$. *Control Parameters* provide the power take-off mechanism and are usually variable parameters, capable of being tuned to match the wave environment; these are represented by a vector $\boldsymbol{J}$. The number of components in $\boldsymbol{G}$ and $\boldsymbol{J}$ will not usually be the same and will be dependent upon the structure of the device and complexity of the power take-off system. The purpose of *Design* is to determine the geometrical parameters $\boldsymbol{G}$ and some measure of the control parameters $\boldsymbol{J}$. The purpose of *Control* is to make the device run efficiently, in some sense, perhaps employing a better measure of $\boldsymbol{J}$ once it has been built.

Although the division with $\boldsymbol{G}$ and $\boldsymbol{J}$ is convenient to employ, it is not definitive and there is an intermingling of parameters at the design stage. Attention is restricted initially to a device of stipulated geometry acting in a regular wave field, then design is considered from a hydrodynamic perspective and finally, more general aspects of control are discussed.

3.6.1 Tuning and Bandwidth

The shortcoming of the optimal control approach is that it does no attempt to include a model of the power take-off mechanism; it acknowledges that a power take-off mechanism is necessary but assumes that it is a black box that can always be adjusted to ensure maximum power absorption. Thus it makes no reference to the equation that governs the device motion or to the contribution made by the external force. It has been the practice thus far to present the mean power, and other related quantities, as functions of the angle of incidence parameter β; this dependency is understood in the present discussion but not explicitly stated.

By analogy with the expression for the radiation force $F_R(t)$ in Eqs. (3.14) and (3.15), write the external force $F_{ext}(t)$ as

$$F_{ext}(t) = Re\left\{-\overline{Z_E}(\omega)\mathbb{U}\, e^{-i\omega t}\right\} \qquad Z_E(\omega) = B_E(\omega) + i\omega A_E(\omega)\,, \tag{3.40}$$

where $Z_E(\omega)$ may be described as the mechanical impedance and $\mathbb{U}$ is the usual complex velocity, i.e. $\mathbb{U} = -i\omega\xi$; this single mode formulation is readily extended to a multi-mode motion. Consider the equation of motion in the form Eq. (3.20) and substitute for $F_{ext}(t)$ from Eq. (3.40), to give the complex velocity and displacement as

$$\mathbb{U} \;=\; \frac{\mathbb{X}}{\overline{Z_T}(\omega) + \overline{Z_E}(\omega)} \;=\; -i\omega\xi\,. \tag{3.41}$$

The instantaneous rate of working of the external force is $F_{ext}(t)U(t)$ and the instantaneous output power is given by $P_{ext}(t) = -F_{ext}(t)U(t)$, with the minus sign providing the link between the rate of working and the power absorbed. Employing Eqs. (3.40) and (3.41), the mean output power becomes

$$\mathcal{P}_{ext} = -\left\langle F_{ext}(t)U(t)\right\rangle = \frac{1}{4}\left(Z_E + \overline{Z_E}\right)\left|\mathbb{U}\right|^2 = \frac{\left|\mathbb{X}\right|^2}{4}\frac{\left(Z_E + \overline{Z_E}\right)}{\left|\overline{Z_T} + \overline{Z_E}\right|^2}\,, \tag{3.42}$$

with Z_T regarded as fixed, the maximum value of this quantity occurs when

$$Z_E = \overline{Z_T} \tag{3.43}$$

to give P_{max} as

$$\mathcal{P}_{max} = \max\left\{\mathcal{P}_{ext}\right\} = \frac{\left|\mathbb{X}\right|^2}{8B} \qquad \text{when } \mathbb{U} = \frac{\mathbb{X}}{2B}\,. \tag{3.44}$$

This is agreement with the optimal result Eq. (3.30) and the approach can be extended to a single body in more than one mode of motion and provides confidence in the optimal results derived earlier. The control defined by Eq. (3.40),

with optimal value Eq. (3.43), is usually called *Complex Conjugate Control*. The structure of the control can be seen by forming the ratio of the two terms in Eqs. (3.42) and (3.44) and then employing (3.41) to give

$$\frac{\mathcal{P}_{ext}}{\mathcal{P}_{max}} = 2B\frac{\left(Z_E + \overline{Z_E}\right)}{\left|\overline{Z_T} + \overline{Z_E}\right|^2} = \left\{1 - \frac{\left|Z_T - \overline{Z_E}\right|^2}{\left|Z_T + Z_E\right|^2}\right\}, \tag{3.45}$$

in which the importance of the relationship between Z_T and Z_E is clearly seen. It is clearly insufficient to restrict Z_E to contain only a damping term, corresponding to Z_E being real. Both real and imaginary parts of Z_E will be important but the degree of importance will depend upon the relative magnitudes of the real and imaginary parts of Z_T. An interesting study on the application of complex control methods to the Salter Duck has been conducted by Nebel (1992) and describes both the strengths and pitfalls of the method.

The optimal results in Section 3.5 show the best that can be achieved, whereas the output power is dependent upon the form of the power take-off. Thus the maximum Eq. (3.44) is dependent upon the form of F_{ext} in Eq. (3.40) and a different expression may not produce as much output power. In terms of the control vector $\boldsymbol{J}$ identified earlier, Eq. (3.40) is equivalent to the form

$$\boldsymbol{J} = \left(Re\{Z_E\}, \mathrm{Im}\{Z_E\}\right) \tag{3.46}$$

and the process adopted is equivalent to the following optimisation problem: determine P_{max} from

$$\mathcal{P}_{max} = \max\left\{\mathcal{P}_{ext}\left(\omega; \boldsymbol{J}\right)\right\} \tag{3.47}$$

for unknown $\boldsymbol{J}$, with information from Eqs. (3.40), (3.42) and (3.46). Equivalently, and more usually, this would be formulated using the capture width $L(\omega; \boldsymbol{J})$ from Eq. (3.5), since this does not depend upon the incident wave amplitude.

Suppose that the system is tuned to provide the maximum mean output power at a chosen frequency ω_T, dependent upon the wave climate. This enables $\boldsymbol{J}$ to be determined, denote it by $\boldsymbol{J_0}(\omega_T)$ and consider as fixed. The *Bandwidth* is then defined by the function $\mathcal{L}\left(\omega; \boldsymbol{J_0}(\omega_T)\right)$ and this provides the variation of the capture width with ω for a system tuned to ω_T. It does not mean that the maximum value of L occurs at ω_T, since the dependency upon ω in the hydrodynamic coefficients may be dominant.

Examples of bandwidth curves are shown in Fig. 3.7 and are taken from a numerical study of the Bristol Cylinder by Thomas and Ó Gallachóir (1993). This device belongs to the *Third Generation* category and power is extracted in two modes of motion; in the present model the power take-off is affected via taut extensible cables. A full description of device, together with the modelling approach and an experimental study is given by Davis et al. (1981), with ample references contained therein. The calculations were performed for a device of $6\,m$ radius, operating in $42\,m$ of water and with a clearance above the cylinder of

3 *m*. A two-dimensional model was employed and so the curves denote hydrodynamic efficiency.

Three curves are shown, indicating tuning for waves of period 8 *s*, 10 *s* and 12 *s*, and the frequency measure is the non-dimensional quantity $\nu = \omega^2 h / g$. The maximum hydrodynamic efficiency curve is also shown and this is seen to be achieved at each tuning frequency. It is clear that the bandwidth narrows as the tuning period increases, with a corresponding increase in wavelength. This is because this device performs best and very efficiently when the particle paths are circular, as for deep-water waves, and becomes less efficient as the eccentricity of the elliptical paths increases. This is confirmed by the 8 *s* bandwidth curve being the widest and the 12 *s* curve being the narrowest. Thus the bandwidth variation parameter is an important consideration in this example and this is a general conclusion. The characteristics of the bandwidth are dependent mainly upon the mode of motion and geometry of the device and some devices may be broad-banded whereas others will be narrow-banded. However, as shown very clearly by this example, it is possible for a device to possess a broad bandwidth in some potion of the frequency spectrum and a narrow bandwidth in another part.

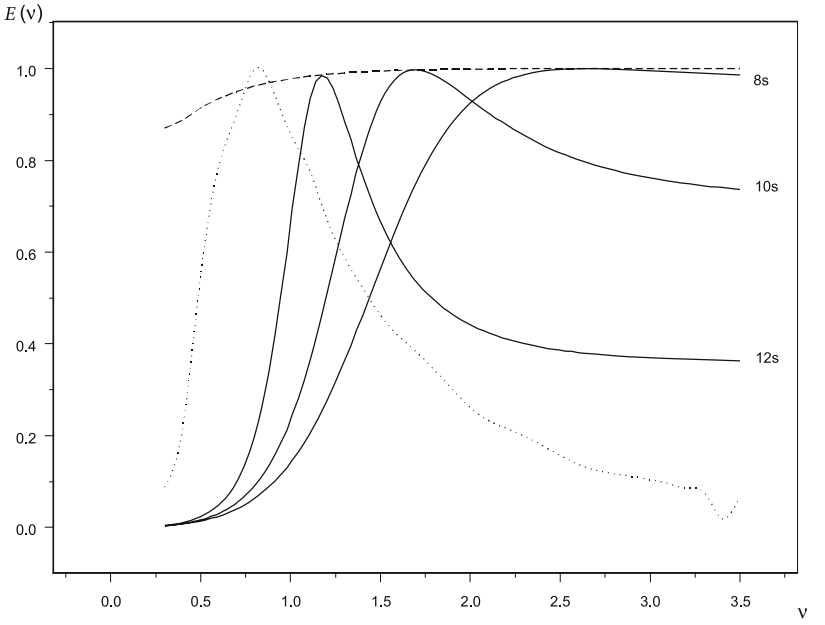

Fig. 3.7. Typical bandwidth curves for the Bristol Cylinder, showing the variation of hydrodynamic efficiency E with non-dimensional frequency ν for three tuning frequencies (solid lines). The maximum efficiency curve (broken line) and the South Uist resource curve from Fig. 3.2 (dotted line) are also shown

3.6.2 Design

A normalised form of the South Uist spectrum presented in Fig. 3.2 is also shown as a dotted line in Fig. 3.7, with the normalisation achieved by dividing the power spectrum density by the maximum power level in the spectrum. It is included to show how the target resource interacts with the modelling approach and to help identify where the device must operate within a particular spectrum. Thus the performance of a device must in some way be targeted at a representative site spectrum or spectra; identifiable mechanisms to meet this requirement include tuning to an appropriate frequency or some methodology of influencing the device bandwidth. These are approaches based upon the idea of control discussed above but control does not provide the only mechanism since any flexibility in the geometrical structure of the device, summarized by the vector $\boldsymbol{G}$, may also possess a potential influence. Including the geometrical parameters incorporates the concept of design, albeit only from a hydrodynamic perspective and this is an acknowledged limitation of the present approach. Device design is an evolutionary process and will change necessarily with gains in relevant knowledge and expertise, whether they are from improved mathematical models, novel laboratory experimental studies or the availability of improved construction materials. However, some convergence of ideas is necessary because not all devices can be built at demonstration or prototype stage and an assessment of design and performance characteristics will be required.

It is possible to make some preliminary comments about two particular hydrodynamic aspects of device design. The first is that it is generally accepted that WECs that are good absorbers of wave energy are also good wave generators, i.e. if the body is forced to move in its prescribed mode of motion, with the water initially at rest, then a uni-directional wavetrain will be generated. An accompanying constraint is that the amplitude of the forced body motion should be comparable to the amplitude of the generated wave for an efficient wave generator, consistent with the employment of modelling within the diffraction regime.

The second point is that most first and second generation wave energy devices have either been strongly site specific or site independent. Usually the distinction is dependent upon whether the device is shore mounted or a small offshore device. A typical shore-mounted, first generation device is an OWC that has been constructed to utilise a natural shore site such as a gully, whereas the general offshore second-generation device is anticipated as working well over a range of sea conditions and sites. The difference between the two cases is associated essentially with the bandwidth: site specific devices usually have a narrow bandwidth, whereas offshore devices are intended to have, but may not possess, a much broader bandwidth. This is seen in Fig. 3.2, which illustrates the difference in the magnitude of the maximum power level and the spectral width between the offshore and onshore resource at Pico. However, as potential offshore sites are identified by criteria established from wave resource assessment studies, then even seemingly site-independent WECs will require change to optimise the power generation. These changes will be dictated by factors such as body response amplitudes to dominant energy frequencies and constraints imposed by

power take-off mechanisms. It is important to possess models that can respond to such demands.

Consider a device operating in a single sea state, characterised by the energy density $S_f(f)$ or the power density $P(f)$. The total power in the incident spectrum is $P_\infty = \int_0^\infty P(f)\,df = \rho g \int_0^\infty S_f(f)\,c_g(f)\,df$. In assessing the power absorbing capability of a particular device at a given site, there must be a recognition that only a portion of this power spectrum may be considered attainable and thus targeted. This introduces the targeted power in the spectrum PT defined by

$$P_T = P\left[f_1, f_2\right] = \rho g \int_{f_1}^{f_2} S_f(f)\,c_g(f)\,df \,. \tag{3.48}$$

The physical frequency f (in *Hz*) may not be the best measure of frequency for modelling purposes, as shown in the text accompanying Fig. 3.7, and the most common alternative is the radian frequency ω. Other useful options are the non-dimensional frequency measures $\nu = \omega^2 h/g$ and $\omega^2 D/g$, with the former being particularly appropriate in finite depth or shallow-water applications and the latter in deep water; this being due to the appropriate choice of length-scale chosen for non-dimensionalisation in each case. To cover all possibilities, write P_T in the form

$$P_T = P\left[\mu_1, \mu_2\right] = \int_{\mu_1}^{\mu_2} P_\mu(\mu)\,d\mu \qquad P_\mu(\mu) = \rho g c_g\, S_\mu(\mu)\,\frac{d\mu}{df}, \tag{3.49}$$

and which encompasses all such applications by allowing μ to be a generic measure of frequency with the physical measure corresponding to $\mu = f$. An example is given by comparison of the South Uist spectrum shown in Figures 3.2 and 3.7; Figure 3.7 shows the range $0.3 \le \nu \le 3.5$ and this corresponds to the range $0.0042 \le f \le 0.144$ in Fig. 3.2. The targeted part of the spectrum has a mean power level of 43.2 *kW/m*, in contrast to the value of 47.8 *kW/m* quoted earlier for the full spectrum.

The simplest strategy to widen the bandwidth of a device with fixed stipulated geometry is to maximise the capture width; this is achieved by defining the control parameter vector $\boldsymbol{J}_1$ by

$$\mathcal{L}_1(\boldsymbol{J}_1) = Max\left\{\frac{1}{\mathcal{L}_T}\int_{\mu_1}^{\mu_2} \mathcal{L}\left(\mu;\boldsymbol{J}(\mu)\right)\,d\mu\right\}, \qquad \mathcal{L}_T = \int_{\mu_1}^{\mu_2} \mathcal{L}_{max}\left(\mu\right)\,d\mu \,. \tag{3.50}$$

As the denominator L_T corresponds to the area under the broken line in Fig. 3.7, the maximum value of $\mathcal{L}_1(\boldsymbol{J})$ is unity and the resultant bandwidth curve from this measure is $\mathcal{L}(\mu, \boldsymbol{J}_1)$. The optimisation process will generally require numerical procedures and the complexity will depend upon the number of control parameters contained within $\boldsymbol{J}$. However, the definition of L_T is associated with a constant scaling factor and needs to be calculated only once. Such an approach

corresponds to a de-tuning as the strategy for parameter choice attempts to move away from the influence of resonance.

The principal shortcoming of Eq. (3.50) is that although it addresses perceived deficiencies in bandwidth, it does not ensure that any improvement in bandwidth occurs in a particular part of the frequency range. This is illustrated in Fig. 3.7, where the dotted line shows a normalised representation of the resource and it is clear that any improvement in bandwidth should match the region where the resource is greatest. To address this deficiency, consider the measure

$$\mathcal{L}_2(\boldsymbol{J}_2) = Max\left\{\frac{1}{P_T\mathcal{L}_T}\int_{\mu_1}^{\mu_2} P_\mu(\mu)\,\mathcal{L}\left(\mu;\boldsymbol{J}(\mu)\right)d\mu\right\}, \tag{3.51}$$

with the optimizing value $\boldsymbol{J_2}$ and corresponding bandwidth function $\mathcal{L}(\mu,\boldsymbol{J}_2)$. It is clear that the power density provides a weighting that moves the bandwidth towards the targeted regions of highest power. Note that the scaling factor $P_T\mathcal{L}_T$ is optional, as it does not contain variable parameters but can be useful from a practical numerical perspective.

Both Eqs. (3.50) and (3.51) describe a de-tuning approach to improve bandwidth for a stipulated body geometry but neither takes body parameters into account except in the calculation of the hydrodynamic coefficients. This deficiency can be overcome by including the body parameter vector $\boldsymbol{G}$ in the set of unknowns and thus Eq. (3.51) is extended to produce the final measure

$$\mathcal{L}_3(\boldsymbol{G}_3,\boldsymbol{J}_3) = Max\left\{\frac{1}{P_T}\int_{\mu_1}^{\mu_2} P_\mu(\mu)\,\mathcal{L}\left(\mu;\boldsymbol{G}(\mu),\boldsymbol{J}(\mu)\right)d\mu\right\}, \tag{3.52}$$

with accompanying bandwidth $\mathcal{L}(\mu,\boldsymbol{G}_3,\boldsymbol{J}_3)$. A variant on this is

$$\hat{\mathcal{L}}_3(\boldsymbol{G}_3,\boldsymbol{J}_3) = Max\left\{\frac{1}{P_T}\int_{\mu_1}^{\mu_2} P_\mu(\mu)\,\hat{\mathcal{L}}\left(\mu;\boldsymbol{G}(\mu),\boldsymbol{J}(\mu)\right)d\mu\right\}, \tag{3.53}$$

where $\hat{\mathcal{L}}$ is the non-dimensional capture width as in Eq. (3.34) and its importance identifies the presence of the physical width of the device in the capture process. The quantity L_T does not appear in Eqs. (3.52) or (53), since this will depend upon $\boldsymbol{G}$; it may involve considerable effort in calculation and not provide the best strategy.

The measures in Eqs. (3.50) – (3.52) were first employed by Thomas and Ó Gallachóir (1993) in attempt to provide a design model for the Bristol Cylinder. Figure 3.8 shows the equivalent two-dimensional forms of the L_1, L_2 and L_3 measures for the Bristol Cylinder, for which a measure of fundamental performance is provided by the bandwidth curves in Fig. 3.7. The dotted line shows the power density of the resource in Figures 3.2 and 3.7; this may be considered to be the target. As expected, an increasing improvement of fit is provided by L_1, L_2 and L_3 respectively, with the same fixed geometry of Fig. 3.7 being employed in L_1 and L_2.

The improvement obtained by targeting the resource is clear and illustrates an important aspect of design, albeit from a hydrodynamic perspective. Newman (1979) also employed a particular form of Eq. (3.52) in his paper on the optimal performance of elongated bodies discussed in Section 3.5.4; the result that the body length should be equivalent to the dominant wavelength of the incident waves is based upon a selected set of calculations equivalent to a less rigorous optimisation process than that of Eq. (3.52).

A key requirement in these approaches is that an accurate hydrodynamic model is available to determine the capture width $\mathcal{L}(\nu, \boldsymbol{G}, \boldsymbol{J})$. It is thus necessary to be able to determine the hydrodynamic coefficients to an acceptable degree of accuracy for the numerical optimisation process to be feasible. Such an approach also requires the numerical evaluation to derivatives and corresponds usually to a requirement of at least one order of magnitude of accuracy better than if the coefficients were employed for the equation of motion alone. Such considerations place stringent conditions upon the numerical methods described in Chapter 5. In addition, when performing a numerical investigation to determine optimal values of $\boldsymbol{G}$ and $\boldsymbol{J}$, there is a need to impose constraints representative of the permissible physical parameter range. These strategies must also be implemented numerically but this does have one advantage: it is then relatively easy to bound any of the design parameters into specified ranges.

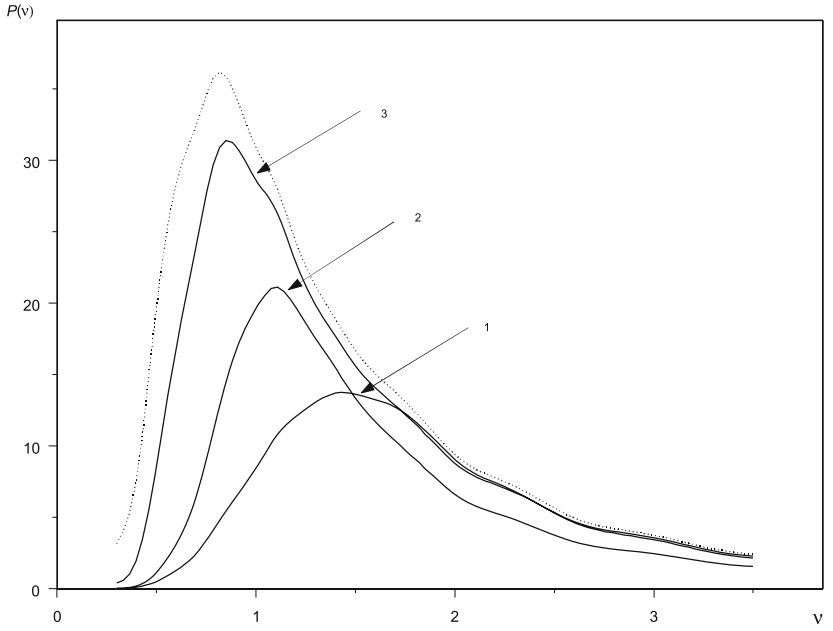

Fig. 3.8. The variation of captured power density $P(\nu)$ with non-dimensional frequency ν for the Bristol Cylinder following implementation of optimisation strategies Eqs. (3.50) – (3.53) (solid lines) with the target South Uist resource (dotted line)

The approach described above targets the device to a particular power spectrum but is not complete for design. There may be many varying sea states that need to be considered and any optimisation process should address this issue. It may well provide an important filtering process in identifying whether or not the device can perform across a variety of sea-states.

3.6.3 Control Strategies

Suppose that the device has been constructed and installed, subject to whatever set of criteria which have been utilised. The question now arises: how should it be controlled to operate most efficiently? It is salient to make some preliminary remarks before attempting to address this difficult question.

The methodologies described in the previous two subsections are based upon an approach embedded in the frequency domain. This relies upon a representation of the typical spectra in Fig. 3.2 in terms of the series of harmonic functions in Eqs. (3.3) and (3.4), together with all accompanying ensuing approximations and caveats. However, the typical physical wave field is shown in Fig. 3.3 and the wave record suggests that frequency domain analysis, via Eq. (3.3), may not provide an acceptable method of controlling the device when relatively large individual waves occur in what may be considered to be at most a moderate sea. Another important consideration is the design and operation of the power take-off mechanism, which may not operate in a harmonic manner and require an appropriate description as a function of time that cannot be incorporated into Eq. (3.17).

These issues may seem to reduce to a comparison between the single-frequency equation of motion in Eq. (3.17) and its time-dependent form Eq. (3.22), or perhaps to a more general comparison of the relative strengths of frequency and time domain modelling. The time-dependent form will provide flexibility in the operation of the power take-off but it remains an equation that is valid only within the confines of linear wave theory and employs coefficients that are obtained using frequency domain modelling. In practice, the relative merits are more concerned with intent: frequency domain models are very useful in determining fundamental device properties and in design studies but control can only be enforced with a time-domain model.

The discussion in Section 3.6.1 considers those aspects of control associated with regular waves and a harmonic power take-off system. Attention is now directed towards a particular aspect of hydrodynamic control, introduced by Budal and Falnes (1980) for point absorbers and known as *Latching*. Consider the heaving buoy shown in Fig. 3.4, with horizontal dimensions sufficiently small to be considered as a point absorber and tuned optimally for maximum power in a regular sea. The tuning condition, capture width and displacement amplitude are given by Eqs. (3.30), (3.32) and (3.33) respectively. For a small device, the Froude-Krylov approximation is valid and the exciting force $\mathbb{X}$ may be obtained by integrating the pressure due to incident wave over the device. This gives a force that is in phase with the incident waves and with magnitude proportional to the radius of

the device. The general tuning condition demands that the body velocity is in phase with the exciting force, which means that the body displacement lags the surface wave elevation by $\pi/2$. As the radius decreases, the displacement amplitude will increase to a value that cannot be achieved without breaking modelling or physical constraints. In addition, the constrained optimisation approach leading to Eq. (3.37) requires an increase in damping that may not be desirable or achievable within the power take-off system.

Latching was conceived to recognise and address these concerns while retaining the small-volume attractiveness of point absorbers. It is easiest described schematically and Fig. 3.9 is very similar to the original figure presented by Budal and Falnes.

The two curves in Fig. 3.9 show the displacement of the device (solid curve) and a representative incident wave motion (dotted line); this is only intended as a schematic and the exact phase relationship between the two motions is given by the optimal criterion in Eq. (3.30). This figure demonstrates a generic latching strategy that immediately halts the motion of the device at some point in the cycle by an appropriate controlling force $F_{ext}(t)$. As the instantaneous power is $F_{ext}(t)U(t)$, the device cannot generate power when it is fixed and will not do so until released. This occurs when it is considered appropriate to generate power again. This approach will avoid very large displacement amplitudes but the resulting body motion is no longer harmonic and so the time dependent equation Eq. (3.22) must be used to describe the motion. Greenhow and White (1997) employed this approach for a heaving point absorber device in regular waves to confirm the original concepts.

The latching control strategy is sub-optimal and the method of implementation, such as the location of fix-and-release points, belongs to the user. Although the method is easiest explained for a regular wavetrain, it is essentially an output control upon the time-dependent form of the equation of motion. It is thus applicable

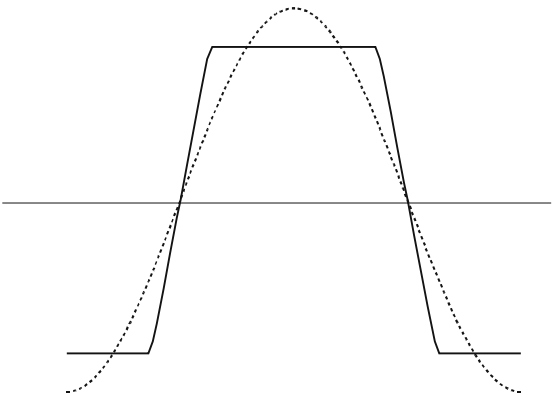

Fig. 3.9. Generic latching strategy, showing desired displacement (heavy solid line) against sinusoidal time dependency (broken line)

in any incident sea and it is straightforward to adapt the concept illustrated in Fig. 3.9 to the time series in Fig. 3.3. However, its use depends upon an accurate calculation of the hydrodynamic coefficients and an efficient and accurate algorithm to evaluate the convolution integral. Possible strategies for heaving point absorbers in irregular seas are considered by Barbarit, Duclos and Clément (2004) and for motions of a more general device by Barbarit and Clément (2006). The second paper discusses evaluation of the convolution integral and on extending such techniques to more general applications. A general review on control strategies and their applications is given by Falnes (2001).

3.7 The Oscillating Water Column

OWCs represent the class of devices that have received the greatest collective development, with perhaps the two best known sites being on the islands of Islay off the west coast of Scotland and Pico in the Azores. Floating or sea-bed devices tend to have been developed on an individual basis with research effort targeted at particular needs, whereas OWCs operate using similar technologies and possess similar requirements. In addition the great majority of OWCs is shore-mounted and this holds for devices either installed or in the prototype and development stages and whether of stand-alone design or integrated into a breakwater. Attention is directed towards the shore-mounted devices. Note that the two mentioned examples (LIMPET in Islay and the Pico plant) are described in Chapter 7. A brief description of the principles is presented in this section.

A generic shore-mounted OWC is shown in cross-section in Fig. 3.10. Incident waves induce a time-varying pressure field in the air chamber inside the device and power is extracted via a turbine and generator. The turbine is driven by the varying differential pressure field across it and includes both inhaling and exhaling phases in the wave cycle. A self-rectifying turbine, which rotates in the same direction independent of the direction of flow, is usually employed. Before considering the available modelling techniques for power extraction, it is appropriate to discuss the key features of the device shown in Fig. 3.10 from a hydrodynamic and aerodynamic perspective.

The shape and thickness of the front wall must ensure that the device survives severe weather conditions, particularly those forces associated with wave slamming. Water flowing past the lip may induce vortex shedding and hence rather turbulent flow within the vicinity of the front wall, though this may be mitigated by a circular lip. As the device is shore-mounted, the incident wave-field is likely to be at best weakly nonlinear and the same remark will apply to the pressure field within the chamber. The forced air-flow within the chamber is unlikely to be smooth or laminar and there is the possibility of water droplets suspended within the air. It is clear that although the global operating principle of an OWC is simple, in the sense that it is straightforward to describe, the construction of a good model to described the working principle of an OWC is likely to be a far from trivial task.

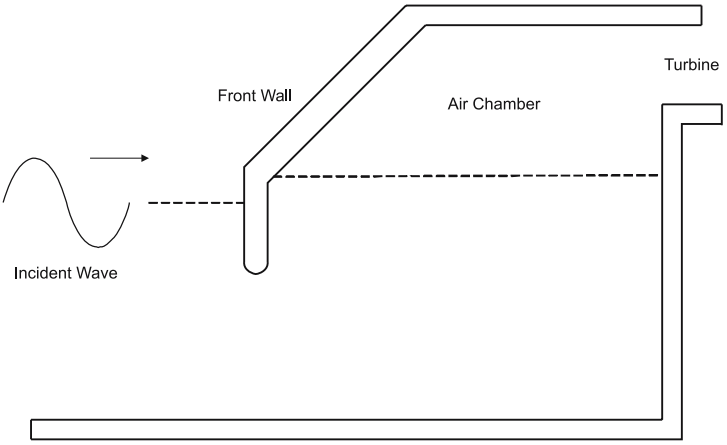

Fig. 3.10. Schematic showing vertical cross-section of shore-mounted OWC

Modelling the hydrodynamic behaviour alone, for the phenomena identified above, is difficult and requires advance numerical techniques. The influence of nonlinearity is considered in the absence of viscosity by Mingham et al. (2003), viscosity and turbulence are included via a k-ε model in a study by Alves and Sarmento (2006). Both of these papers describe two-dimensional studies and this approach is common in shore-mounted OWC modelling, in recognition of the considerable increase in complexity in moving to three-dimensions but also acknowledging that two-dimensional models can provide an important input in the appropriate circumstances. One point to note is that the LIMPET device on the Scottish island of Islay, described in Chapter 7, does not conform to the schematic in Fig. 3.10 and slopes uniformly. For the sake of convenience, Fig. 3.10 is taken to provide the generic form.

A major difficulty is that experimental studies on OWCs are not easy to perform: the hydrodynamic and pneumatic flows require different model scales and the influence of vortex shedding and viscous effects is difficult to infer from small-scale experiments. This makes mathematical and numerical modelling a particularly valuable tool in the development of OWCs. For convenience, the existing models are separated again into those appropriate for the frequency and time domains.

3.7.1 Frequency Domain Modelling

In spite of the reservations identified above concerning the applicability of linear wave theory, most of the modelling of OWCs involving power take-off has assumed that linear wave theory is valid. This should not be interpreted as a severe

deficiency in preliminary modelling; the device must perform most efficiently in small waves and there are many phenomena that cannot be described adequately without an increase in the number of parameters.

The schematic shown in Fig. 3.11 is usually employed for two-dimensional studies and this can be compared readily with the more realistic configuration in Fig. 3.10. There are two main differences, allowing for the turbine to be placed in the roof or in the rear wall. In practice the front wall must possess a considerable thickness, associated with the survivability of the device and with vortex shedding and turbulence, whereas the idealised model has a wall of negligible thickness. The second difference concerns the sloped portion of the upper wall in the installed device and the idealised model retains a vertical wall at the front of the device. These differences are not easy to assess; the practical wall thickness will probably diminish the power incident to the device and the sloped wall may improve the internal air movement. In a preliminary model, both approximations are deemed acceptable.

The fundamental model is due to Evans (1982), who introduced the concept of an oscillating pressure patch on the water surface and equivalent to the interior water surface of an OWC. The original work was for an array of OWCs rather than just an individual device but the limitation to a single device is enforced here. Water wave theory assumes that the pressure on the air-water interface is equal to the air pressure p_a and this is taken usually to be constant. With reference to Fig. 3.11, air outside the chamber will be at atmospheric pressure p_a whereas the surface pressure inside the chamber will take a different value and will change due to the interior conditions in the chamber. If $p_c(t)$ is the air pressure in the chamber, then for harmonic time dependency write

$$p_c(t) = p_a + p(t), \quad p(t) = Re\left\{ \mathbb{P} e^{-i\omega t} \right\}, \tag{3.54}$$

where $p(t)$ is the difference between the chamber pressure and the external atmospheric pressure. The rate of change of the volume inside the chamber is due the

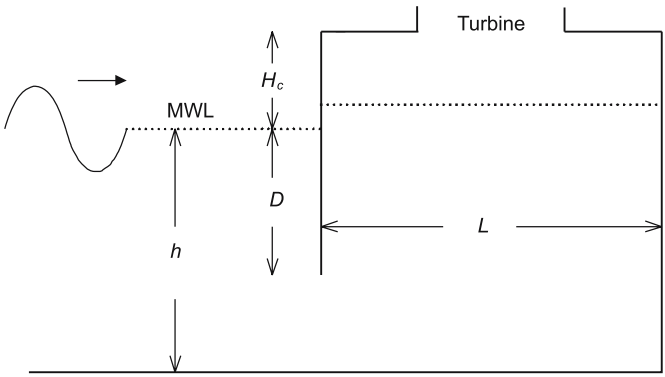

Fig. 3.11. Schematic showing model approximation to Fig. 3.10

change in surface level inside the chamber and can be represented as a volume flux $Q(t)$, measured positive in an upwards direction. In linear theory it can be written as

$$Q(t) = Q_S(t) + Q_R(t) = Re\left\{\left(\mathbb{Q}_S + \mathbb{Q}_R\right)e^{-i\omega t}\right\}, \tag{3.55}$$

associated with the scattered and radiated wave fields respectively and directly analogous to the decomposition in Eq. (3.8) for the forces on a floating body. The analogy is extended by writing $Q_R(t)$ as

$$Q_R(t) = -\left\{A(\omega)\dot{p}(t) + B(\omega)p(t)\right\}, \tag{3.56}$$

where A and B behave very much like the added-mass and damping coefficients encountered previously and so the same notation is employed. Using the representation

$$\mathbb{Q}_R = -\overline{Z}_R(\omega)\mathbb{P}, \quad Z_R(\omega) = B(\omega) + i\omega A(\omega) \tag{3.57}$$

identifies a further analogy with the floating body analysis, this time with Eq. (3.15). As with the floating body, calculation of A and B will depend upon the geometry of the OWC and numerical determination is usually required. At this point it is possible to consider the mean power generated via the optimal approach of Section 3.5; the optimal result for P_{opt} is directly analogous to the floating body result of Eq. (3.30), with $\mathbb{U}$ replaced by $\mathbb{Q}_S$.

The control approach of Section 3.6 requires the power take-off mechanism to be stipulated. Evans assumed that the pressure across the turbine is related to the volume flux of the air inside the chamber and that the two quantities are related by a complex constant of proportionality α. i.e.

$$\mathbb{Q}_S + \mathbb{Q}_R = \alpha\mathbb{P}, \tag{3.58}$$

The mean rate of working of the turbine is $\mathcal{P}_{turb} = \left\langle p_c(t)Q(t)\right\rangle$; utilising the forms in Eqs. (3.54) – (3.58) enables this expression to be written as

$$\mathcal{P}_{turb} = \frac{\left|\mathbb{Q}_S\right|^2}{8B}\left\{1 - \frac{\left|Z_R - \overline{\alpha}\right|^2}{\left|Z_R + \alpha\right|^2}\right\}. \tag{3.59}$$

The conjugate control methods of Section 3.6.1 may now be implemented and the maximum output power $P_{\max}$ occurs when $\alpha = \overline{Z_R}$ giving

$$\mathcal{P}_{max} = \max\left\{\mathcal{P}_{turb}\right\} = \frac{\left|\mathbb{Q}_S\right|^2}{8B} \qquad \text{when} \quad \mathbb{P} = \frac{\mathbb{Q}_S}{2B}. \tag{3.60}$$

This is in agreement with the optimal result in Eq. (3.30) for the floating body and the results in Eqs. (3.44) and (3.45) for the maximum power generated by the external force. The importance of the damping B and the diffraction flow $\mathbb{Q}_S$ are

clear, thus it is essential to be able to determine these quantities accurately and the necessity for efficient and accurate numerical methods is identified again. General numerical methods of industrial standard and employing the boundary element technique would be required to determine the volume fluxes and capture width for a three-dimensional model of the shore-mounted OWC. Applications are given by Lee and Newman (1996) and Brito-Melo et al. (1999), with the latter paper concentrating upon the requisite diffraction flow calculations referenced to the Pico plant.

Attention is now directed at the two-dimensional application in Fig. 3.11. This requires a finite depth model rather than an infinite depth one and the extension from the original work of Evans was provided by Smith (1983). It is often assumed that the oscillating pressure and volume flux will be in phase; thus the constant of proportionality α is real and the complex conjugate control leading from Eqs. (3.59) to (3.60) cannot be enforced, with a corresponding diminution in output power. The resulting hydrodynamic efficiency at the non-dimensional frequency $\nu\,(=\omega^2 h/g)$ is given by

$$\mathcal{E}(\nu) \;=\; 4\frac{h}{L}\frac{\alpha_0}{\sqrt{\nu}}\Bigg/\left[\left(\frac{h}{L}\frac{\alpha_0}{\sqrt{\nu}}+\tilde{B}\right)^2+\tilde{A}^2\right], \tag{3.61}$$

dependent upon the frequency and geometry; α_0 is real and a non-dimensional form of α and $\tilde{A}, \tilde{B}$ are non-dimensional forms of the coefficients in Eq. (3.56). This expression possess a maximum value of

$$\mathcal{E}_{max}(\nu) \;=\; \frac{2}{1+\sqrt{\tilde{A}^2+\tilde{B}^2}}, \qquad \text{when } \alpha_0 = \frac{L\sqrt{\nu}}{h}\sqrt{\tilde{A}^2+\tilde{B}^2} \tag{3.62}$$

and this is a maximum value rather than an optimal one, since it depends upon a particular choice of the power take-off parameter. A physical implementation requires the values of the hydrodynamic coefficients $\tilde{A}$ and $\tilde{B}$, these can be obtained accurately and efficiently by the method of Evans and Porter (1995).

In terms of the design approach described in Section 3.6.2, Eq. (3.60) is obtained from Eq. (3.59) by specifying the geometrical parameter vector $\boldsymbol{G} = (D, L)$ and varying the complex control parameter $\boldsymbol{J} = (\alpha)$. If the device is tuned to the frequency ν_T for fixed $\boldsymbol{G}$, then α is obtained from the condition in Eq. (3.60) and the corresponding bandwidth curves $\mathcal{E}\left(\nu;\boldsymbol{J}_0(\nu_T)\right)$ are obtained from Eq. (3.59).

For this two-dimensional geometry, Evans et al. (1995) combined the techniques introduced by Thomas and O Gallachoir (1993), outlined in Section 3.6.2, with the rapid and accurate numerical technique of Evans and Porter (1995) to maximise the function

$$\mathcal{E}_3(\boldsymbol{G}_3,\boldsymbol{J}_3) = Max\left\{\frac{1}{P_T}\int_{\nu_1}^{\nu_2} P_\nu(\nu)\,\mathcal{E}\left(\nu;\boldsymbol{G}(\nu),\boldsymbol{J}(\nu)\right)d\nu\right\} \tag{3.63}$$

for the Pico power spectrum shown in Fig. 3.2. (The subscript $_3$ is used in this expression to denote a direct analogy with the capture width / hydrodynamic efficiency function of Eq. 3.52). A constrained numerical optimisation scheme was implemented to ensure that the parameters remained within acceptable bounds and the findings suggested that the device could achieve a hydrodynamic efficiency of just over 90 % for the approach adopted. Of greater interest are the predicted dimensions of the optimal device values in comparison with those previously chosen for the Pico plant. The chamber length L was very similar for the predicted and chosen values but there was a slight difference in the values of the barrier depth D, with the numerical approach suggesting a value slightly greater than that chosen. This parameter helps to target the requirements of the spectrum.

The hydrodynamic efficiency value quoted above is derived from a model that matches the hydrodynamics reasonably well but does not provide an accurate description of the chamber aerodynamics or the power take-off mechanism. A discussion of these failings is given by Sarmento and Falcão (1985), who also identify the difficulty of performing scale experiments with OWCs.

To obtain a better understanding of the aerodynamics in the chamber, and hence of the hydrodynamic-aerodynamic coupling, follow the approach outlined originally by Sarmento, Gato and Falcão (1990) and employ the notation of Eqs. (3.54) and (3.55). Note that the aerodynamics of air turbines and their application to OWCs are assessed in detail in Chapter 6. The chamber is taken to possess an arbitrary width W for convenience but the modelling is genuinely two-dimensional and the choice $W=1$ is permissible. Denote the volume of air in the chamber and the water volume contained within the chamber and above the barrier by $V_c(t)$ and $V_w(t)$ respectively. With reference to Fig. 3.11, the still water values of these quantities are LH_cW and LDW; they are related at all times by

$$V_w + V_c = L\left(D+H_c\right)W . \tag{3.64}$$

From Eqs. (3.55) and (3.64)

$$\frac{dV_w}{dt} = Q(t) = Q_S(t) + Q_R(t) = -\frac{dV_c}{dt} . \tag{3.65}$$

If $\rho_c(t)$ and ρ_a are the density of the air inside and outside the chamber respectively, then the adiabatic gas law gives

$$\frac{\rho_c(t)}{\rho_a} - 1 = \frac{1}{\gamma}\left(\frac{p_c(t)}{p_a} - 1\right) = \frac{p(t)}{\gamma} , \tag{3.66}$$

where γ is the usual ratio of specific heats and Eq. (3.66) is valid under the assumption that both sides of the identity are small, i.e. the pressure and density inside the chamber do not vary much from their ambient values. The air mass in the

chamber $M_c(t)$ can only change by a non-zero flux across the turbine, measured positive in an outward direction, and thus

$$\frac{dM_c}{dt} = \frac{d}{dt}\left(\rho_c V_c\right) = -\rho_a Q_t(t), \tag{3.67}$$

where $Q_t(t)$ is the volume flux at the turbine. Now combine Eqs. (3.64) – (3.67) to yield $Q_t(t)$ in the form

$$Q_t(t) = \frac{\rho_c(t)}{\rho_a} Q(t) - \left[L\left(D + H_c\right)W - V_w(t)\right]\frac{1}{\gamma p_a}\frac{dp}{dt}. \tag{3.68}$$

This relationship couples the hydrodynamic and aerodynamic domains and is weakly nonlinear; a linearised form can be obtained easily by replacing $\rho_c(t)$ by ρ_a and $V_w(t)$ by LDW in Eq. (3.68),

$$Q_t(t) = Q(t) - \frac{LH_cW}{\gamma p_a}\frac{dp}{dt}. \tag{3.69}$$

In the absence of aerodynamic considerations, $Q_t(t)$ and $Q(t)$ would be the same and this is the approximation applied in the original Evans (1982) model. Both Eqs. (3.68) and (3.69) show clearly how compressibility in the aerodynamic domain can play an important role and so demands inclusion in the modelling process.

The instantaneous power at the turbine is $p(t)Q_t(t)$ and analogous to Eq. (3.58) it is assumed that

$$Q_t(t) = \alpha p(t), \tag{3.70}$$

with α being real. For known $Q(t)$ the differential pressure $p(t)$ can be determined from the particular integral solution of Eq. (3.69) and hence the instantaneous power $P_{aero}(t) = \alpha p^2(t)$ can be determined. The addition of air compressibility introduces another device parameter, the chamber height H_c, into the geometrical design vector $\boldsymbol{G}$. Weber and Thomas (2000) optimised the quantity

$$\mathcal{E}_{aero}(\boldsymbol{G}_{aero}, \boldsymbol{J}_{aero}) = Max\left\{\frac{1}{WP_T}\left\langle P_{aero}\left(\boldsymbol{G}, \boldsymbol{J}\right)\right\rangle\right\} \tag{3.71}$$

with parameter vectors $\boldsymbol{G} = (D, L, H_c)$ and $\boldsymbol{J} = (\alpha)$ to assess the influence of compressibility. This work was completed for an OWC of fixed width W ($\neq 1$) rather than one of unit width, to enable comparisons to be made with the dimensions of the Pico plant. The findings confirmed the importance of air compressibility, identified earlier by Falcão and Sarmento (1985), and although the hydrodynamic efficiency did not diminish appreciably relative to the hydrodynamic model the parameter values at the maximum efficiency were appreciably different. It may appear from a comparison of Eqs. (3.63) and (3.71) that similar quantities are not being optimised but it is straightforward to show that the approach

adopted for Eq. (3.71) is both analogous to and extends Eq. (3.63). Instead of employing a power density from Fig. 3.2, Eq. (3.71) utilises the time series approach of Fig. 3.3 and Eq. (3.2) with averaging over an appropriate time period. In a sense this is a hybrid method, in which a time series is employed but the difficulties of instantaneous control are not addressed.

An improved model of the power take-off chain requires that a better measure of output power be employed rather than just the aerodynamic power at the turbine and the final approach utilises the mechanical output power. With the exception of the electrical generator this almost corresponds to a complete system analysis. The requirement is to link the hydrodynamic-aerodynamic coupling described above to a description of the mechanical output from the turbine, in a representation possessing physical parameters that may be incorporated into the optimisation process. Once more the input is taken from the specialist literature on the installation of turbines into OWCs and the following model is considered appropriate by Falcão and Justino (1999) for a turbine of Wells type.

The performance of the turbine, subject to justifiable approximation, can be characterised in terms of the non-dimensional flow Φ, pressure Ψ and power Π defined by

$$\Phi = \frac{Q_t}{ND_0^3}, \quad \Psi = \frac{p}{\rho_a N^2 D_0^2}, \quad \Pi = \frac{P_{mech}}{\rho_a N^3 D_0^5}, \tag{3.72}$$

where N and D_0 are the rotational speed and outer diameter of the turbine respectively. These quantities are related by

$$\Phi = f_\Phi(\Psi), \quad \Pi = f_\Pi(\Psi), \tag{3.73}$$

and the unknown functions f_Φ and f_Π are dependent upon the turbine geometry. For the Wells turbine developed for the Pico plant, the relationship f_Φ between Φ and Ψ is linear, confirming Eq. (3.70). The power – pressure relationship f_Π is shown in Fig. 3.12 and this curve possesses an interesting property: following almost linear growth, the power reaches a peak and then decreases rapidly as the turbine stalls. The free parameters to determine the instantaneous mechanical power P_{mech} are now N and D_0, which replace α of the previous formulations.

This extended turbine model has been utilised by Weber and Thomas (2001) to optimise the quantity

$$\mathcal{E}_{mech}(\boldsymbol{G}_{mech}, \boldsymbol{J}_{mech}) = Max\left\{\frac{1}{WP_T}\left\langle P_{mech}(\boldsymbol{G}, \boldsymbol{J})\right\rangle\right\} \tag{3.74}$$

with parameter vectors $\boldsymbol{G} = (D, L, H_c, D_0)$ and $\boldsymbol{J} = (N)$ for the Pico spectrum in Fig. 3.2. The initial work in Eq. (3.63) was an attempt to match the OWC geometry to the shape of the spectrum and is essentially a weighted optimisation problem, as can be seen clearly from the integrand in Eq. (3.63). This is less evident from Eq. (3.74) and there is an important difference, since Eq. (3.74) attempts to match the device parameters to Fig. 3.2, subject to the constraint imposed by

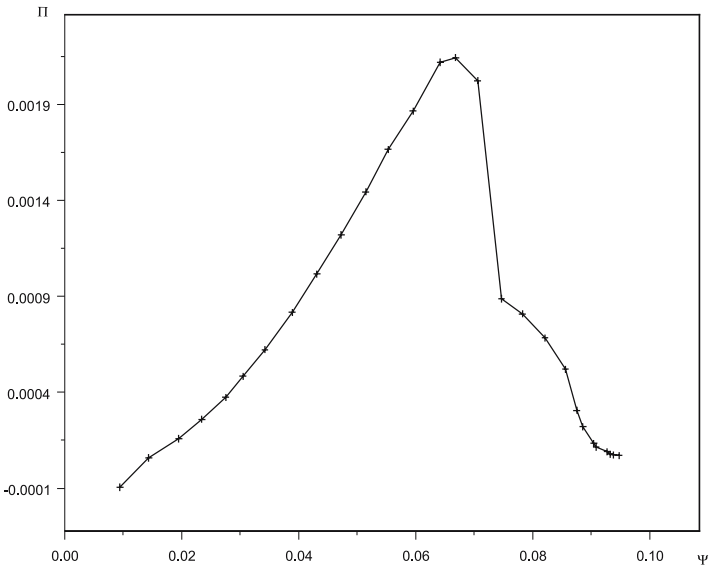

Fig. 3.12. The variation of the non-dimensional turbine power Π with non-dimensional pressure Ψ for the Pico turbine: measured values (×) and interpolation (solid line)

Eqs. (3.72), (3.73), and Fig. 3.12. The resulting output efficiency is much reduced, moving from around 90 % for the hydrodynamic model of Eq. (3.63) to about half that value for the complete optimisation in Eq. (3.74). There are two particular aspects worthy of mention; the first is that the turbine power curve (Fig. 3.12) must match the wave climate in some sense and the second is that complete optimisation must replace partial optimisation in the design process. This work was continued to a target involving multiple sea-states and subsequent local control by Weber and Thomas (2003).

3.7.2 Time Domain Modelling and Control

The frequency domain modelling employs an approach beginning with the hydrodynamics and moving towards the mean mechanical output via an inclusion of the aerodynamics. One of its most important contributions is to provide a reasonable measure of determining the dimensions of a device. Time domain modelling usually assumes that the hydrodynamic problem has been resolved, that the OWC has been constructed and must now be controlled to provide the maximum output within the operating circumstances and range of sea-states. This topic is not within the remit of this review, which is intended to focus upon the hydrodynamic aspects of conversion; power take-off consideration for an OWC is a very specialist topic and is discussed in detail in Chapter 6. However, the work presented thus far

shows how the frequency and time domains interact and a short discussion of those aspects of turbine control applicable to the hydrodynamics is beneficial.

The difference between the frequency and time domain models has already been discussed in Section 3.6 and in the present context, this is epitomised by the information supplied in spectral form (Fig. 3.2) or as a time series (Fig. 3.3). Reference has already been made to Sarmento et al. (1990) and Falcão and Justino (1999) for models of the power take-off but both are control papers involving time domain models with realistic constraints, such as the suitability of by-pass valves to prevent large chamber pressures.

Two other important issues associated with control are identified by Falcão (2002) and Perdigão and Sarmento (2003). The paper by Falcão considers the control of the Wells turbine once the OWC has been constructed, primarily by employing the rotational speed N as the controlling variable and is in keeping with the control modelling described herein. Perdigão and Sarmento consider control of a variable pitch turbine, in contrast to the fixed-pitch assumed so far, and show that appreciable improvements in efficiency can be obtained by this change of design. Both of these papers have implications for future models based upon the hydrodynamic approach.

3.8 Discussion

This brief review has attempted to provide a broad overview of the hydrodynamic theory that underlies the conversion process of the energy possessed by ocean waves into a form more useful to mankind. There are many shortcomings undoubtedly and there are certainly omissions; some are deliberate, others due to the enormous breadth of the field and the accompanying limitation of space. Any review must to certain extent, unintentionally or otherwise, reflect the interests and blinkered perspective of the author and any such perceived deficiencies are acknowledged.

It is hoped that this contribution will encourage those readers whose enthusiasm has been fired by the necessity and certainty of energy extraction from ocean waves will find in this article a good starting point to acquire a working expertise in the discipline. It is proposed that a good basis on wave mechanics and hydrodynamics in the maritime environment can be obtained from the text books in the reference list, followed by an introduction to wave energy via the more advanced texts of Falnes (2002) and the conference proceedings edited by Count (1980). With such an armoury, the other articles cited in this review and the excellent complimentary chapters in this book can be tackled with confidence.

References

Alves M, Sarmento AJNA (2006) Nonlinear and viscous diffraction response of OWC wave-power plants. Proc 6th Eur Wave Tidal Energ Conf. Glasgow, Scotland, pp 11–17

Barbarit A, Clément AH (2006) Optimal latching control of a wave energy device in regular and irregular waves. Appl Ocean Res 28:77–91

Barbarit A, Duclos G, Clément AH (2004) Comparison of latching control strategies for a heaving wave energy device in random sea. Appl Ocean Res 26:227–238

Brito-Melo A, Sarmento AJNA, Clément AH, Delhommeau G (1999) A 3-D boundary element code for the analysis of OWC wave-power plants. Proc 9th Int Offshore Polar Eng Conf. Best, France, pp 188–195

Brooke J (2003) Wave energy conversion. Elsevier

Budal K, Falnes J (1975) A resonant point absorber of ocean-wave power. Nature 257:478–479 [with Corrigendum in Nature 257:626]

Budal K, Falnes J (1980) Interaction point absorbers with controlled motion. In: Count BM (ed) Power from sea waves. Academic Press, pp 381–399

Chaplin RV, Folley MS (1998) An investigation into the effect of extreme waves on the design of wave energy converters. Proc 3rd Eur Wave Energ Conf. Patras, Greece, pp 314–317

Chaplin RV, French MJ (1980) Aspects of the French flexible bag device. In: Count BM (ed) Power from sea waves. Academic Press, pp 401–412

Count BM (ed) (1980) Power from sea waves. Academic Press

Crabb JA (1980) Synthesis of a directional wave climate. In: Count BM (ed) Power from sea waves. Academic Press, pp 41–74

Cummins WE (1962) The impulse response function and ship motions. Schiffstechnik 9:101–109

Davis JP, Finney R, Evans DV, Thomas GP, Askew WH, Shaw TL (1981) Some hydrodynamic characteristics of the Bristol Cylinder. Proc 2nd Int Sym Wave Tidal Energ. Cambridge, England, pp 249–260

Dean RG, Dalrymple RA (1991) Water wave mechanics for engineers and scientists. World Scientific Publishing

Evans DV (1976) A theory for wave power absorption by oscillating bodies. J Fluid Mech 77(1):1–25

Evans DV (1979) Some theoretical aspects of three-dimensional wave-energy absorbers. Proc 1st Symp Wave Energ Util. Gothenburg, Sweden

Evans DV (1980) Some analytic results for two and three dimensional wave-energy absorbers. In: Count BM (ed) Power from sea waves. Academic Press, pp 213–248

Evans DV (1981a) Power from water waves. Ann Rev Fluid Mech 13:157–187

Evans DV (1981b) Maximum wave-power absorption under motion constraints. Appl Ocean Res 3:200–203

Evans DV (1982) Wave-power absorption by systems of oscillating surface pressure distributions. J Fluid Mech 114:481–499

Evans DV, Ó Gallachoir BP, Porter R, Thomas GP (1995) On the optimal design of an Oscillating Water Column device. Proc 2nd Wave Energ Conf. Lisbon, Portugal, pp 172–178

Evans DV, Porter R (1995) Hydrodynamic characteristics of an oscillating water column. Appl Ocean Res 17:155–164

Evans DV, Thomas GP (1981) A hydrodynamical model of the Lancaster flexible bag wave energy device. Proc 2nd Int Sym Wave Tidal Energ. Cambridge, pp 129–141

Falcao AF de O (2002) Control of a oscillating water column wave power plant for maximum production. Appl Ocean Res 24:73–82
Falcão AF de O, Justino PAP (1999) OWC wave energy devices with air flow control. Ocean Eng 26:1275–1295
Falnes J (1980) Radiation impedence matrix and optimum power absorption for interacting oscillators in surface waves. Appl Ocean Res 2:75–80
Falnes J (2001) Optimum control of oscillation of wave-energy converters. Proc 11th Int Offshore Polar Eng Conf. Stavanger, Norway, pp 567–574
Falnes J (2002) Ocean waves and oscillating systems. Cambridge Univ Press
Faltinsen OM (1990) Sea loads on ships and offshore structures. Cambridge Univ Press
Goda Y (2000) Random seas and design of maritime structures, 2nd edn. World Scientific Publishing
Greenhow M, White SP (1997) Optimal heave motion of some axisymmetric wave energy devices in sinusoidal waves. Appl Ocean Res 10:141–159
Jefferys ER (1980) Device characterization. In: Count BM (ed) Power from sea waves. Academic Press, pp 413–438
Justino PAP, Clément AH (2003) Hydrodynamic performance for small arrays of submerged spheres. Proc 5th Eur Wave Energ Conf. Cork, Ireland, pp 266–273
Lee C-H, Newman JN, Nielsen FG (1996) Wave interactions with an oscillating water column. Proc 6th Int Offshore Polar Eng Conf. Los Angeles, USA, pp 82–90
Linton CM, McIver P (2001) Mathematical techniques for wave/structure interactions. Chapman and Hall/CRC
MacIver P (1994) Some hydrodynamic aspects of arrays of wave-energy devices. Appl Ocean Res 16:61–69
Mavrakos SA, McIver P (1997) Comparison of methods for computing hydrodynamic characteristics of arrays of wave power devices. Appl Ocean Res 19:283–291
Mei CC (1976) Power extraction from water waves. J Ship Res 20.63–66
Mingham CG, Qian L, Causon DM, Ingram DM, Folley M, Whittaker TJT (2003) A two-fluid numerical model of the Limpet OWC. Proc 5th Eur Wave Energ Conf. Cork, Ireland, pp 119–125
Nebel P (1992) Maximising the efficiency of wave-energy plant using complex control. J Syst Control Eng. Proc Inst Mech Eng 206:225–236
Newman JN (1962) The exciting forces on fixed bodies in waves. J Ship Res 6:10–17
Newman JN (1976) The interaction of stationary vessels with waves. Proc 11th Symp Naval Hydrodyn. London
Newman JN (1977) Marine Hydrodynamics. MIT Press
Newman JN (1979) Absorption of wave energy by elongated bodies. Appl Ocean Res 1:189–196
Perdigão J, Sarmento AJNA (2003) Overall-efficiency optimisation in OWC devices. Appl Ocean Res 25:157–166
Pizer DJ (1993) Maximum wave-power absorption of point absorbers under motion constraints. Appl Ocean Res 15:227–234
Pizer D, Retzler C, Henderson RM, Cowieson FL, Shaw MG, Dickens B, Hart R (2006) Pelamis WEC – Recent advances in the numerical and experimental modelling programme. Proc 6th Eur Wave Tidal Energ Conf. Glasgow, Scotland, pp 373–378
Pontes MT, Oliveira-Pires H (1992) Assessment of shoreline wave energy resource. Proc 2nd Int Offshore Polar Eng Conf San Francisco, USA, pp 557–562
Randløv P (1996) Final report and annexes to the Offshore wave energy converters (OWEC-1) project. EU Contract No. JOU2-CT93-0394. Danish Wave Power aps
Sarpkaya T, Isaacson M (1981) Mechanics of wave forces on offshore structures. Van Nostrand Reinhold

Sarmento AJNA, Falcão AF de O (1985) Wave generation by an oscillating surface-pressure and its application in wave-energy extraction. J Fluid Mech 150:467–485

Sarmento AJNA, Gato LMC, Falcão AF de O (1990) Turbine-controlled wave energy absorption by oscillating water column devices. Ocean Eng 17:481–497

Smith C (1983) Some problems in linear wave waves. PhD Thesis, Univ of Bristol

Thomas GP, Evans DV (1981) Arrays of three-dimensional wave-energy absorbers. J Fluid Mech 108:67–88 X Thomas GP, Ó Gallachóir BP (1993) An assessment of design parameters for the Bristol Cylinder. Proc 1st Eur Wave Energ Sym. Edinburgh, Scotland, pp 139–144

Tucker MJ, Pitt EG (2001) Waves in ocean engineering. Elsevier

Weber JW, Thomas GP (2000) Optimisation of the hydrodynamic-aerodynamic coupling for an Oscillating Water Column wave energy device. Proc 4th Eur Wave Energ Conf. Aalborg, Denmark, pp 251–259

Weber JW, Thomas GP (2001) An investigation into the importance of air chamber design of an oscillating water column wave energy device. Proc 11th Int Offshore Polar Eng Conf. Stavanger, Norway, pp 581–588

Weber JW, Thomas GP (2003) Some aspects of the design optimisation of an OWC with regard to multiple sea-states and combined object functions. Proc 5th Eur Wave Energ Conf. Cork, Ireland, pp 141–148

Wehausen JV (1971) The motion of floating bodies. Ann Rev Fluid Mech 3:7–268